

Overcoming the Added-Mass Instability in Compressible Fluid-Structure Interaction

Jeff Banks, Bill Henshaw

Lawrence Livermore National Laboratory

Overset Composite Grids and Solution Technology
Dayton, OH, October 16, 2012

Collaborators

Donald Schwendeman

Department of Mathematical Sciences
Rensselaer Polytechnic Institute

Bjorn Sjogreen

Center for Applied Scientific Computing
Lawrence Livermore National Laboratory

Support

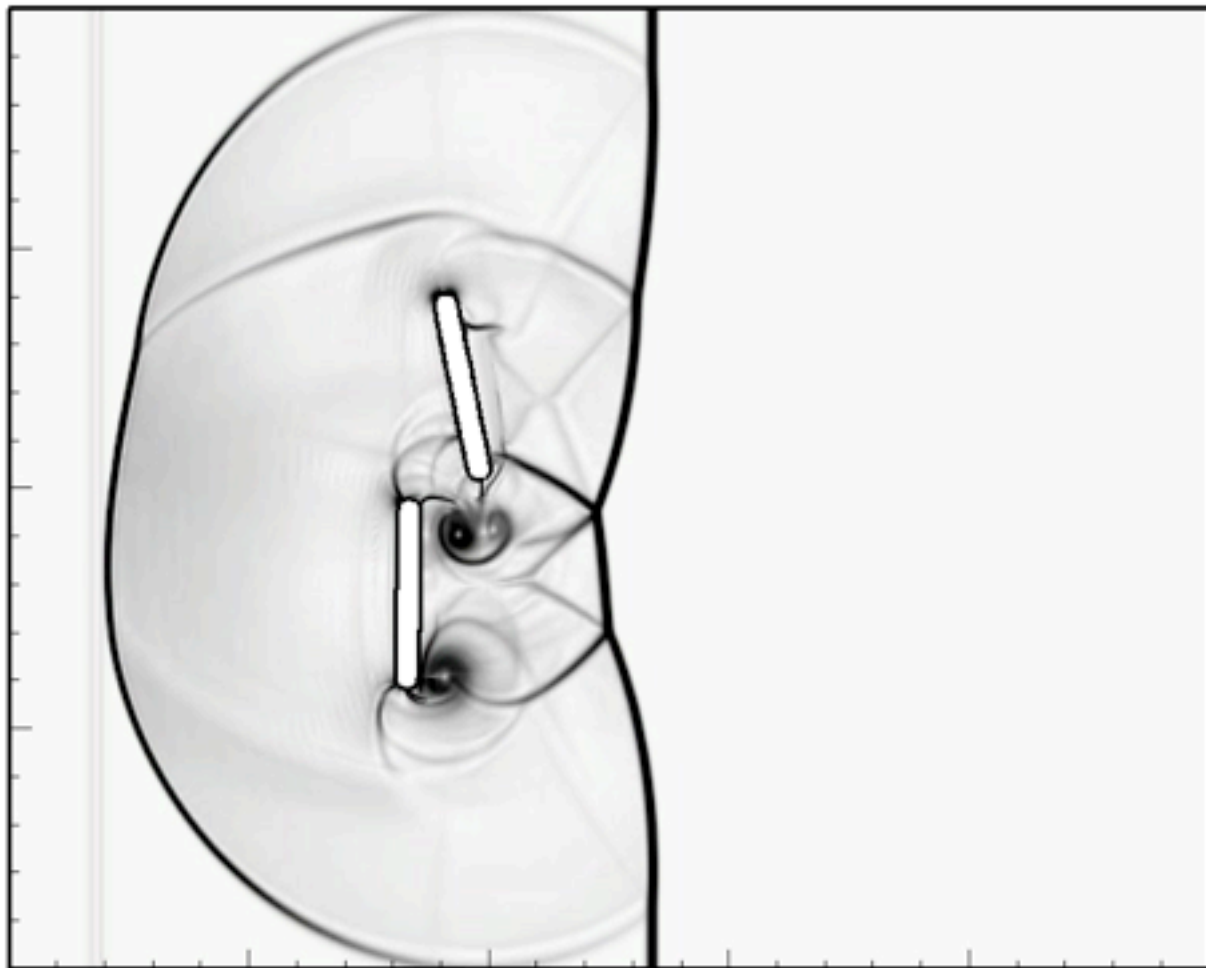
Department of Energy
Office of Advanced Scientific Computing Research
Applied Mathematics Program
Department of Defense
Lawrence Livermore National Laboratory
National Science Foundation

In this work our target applications are high-speed compressible flows with embedded deforming or rigid solids

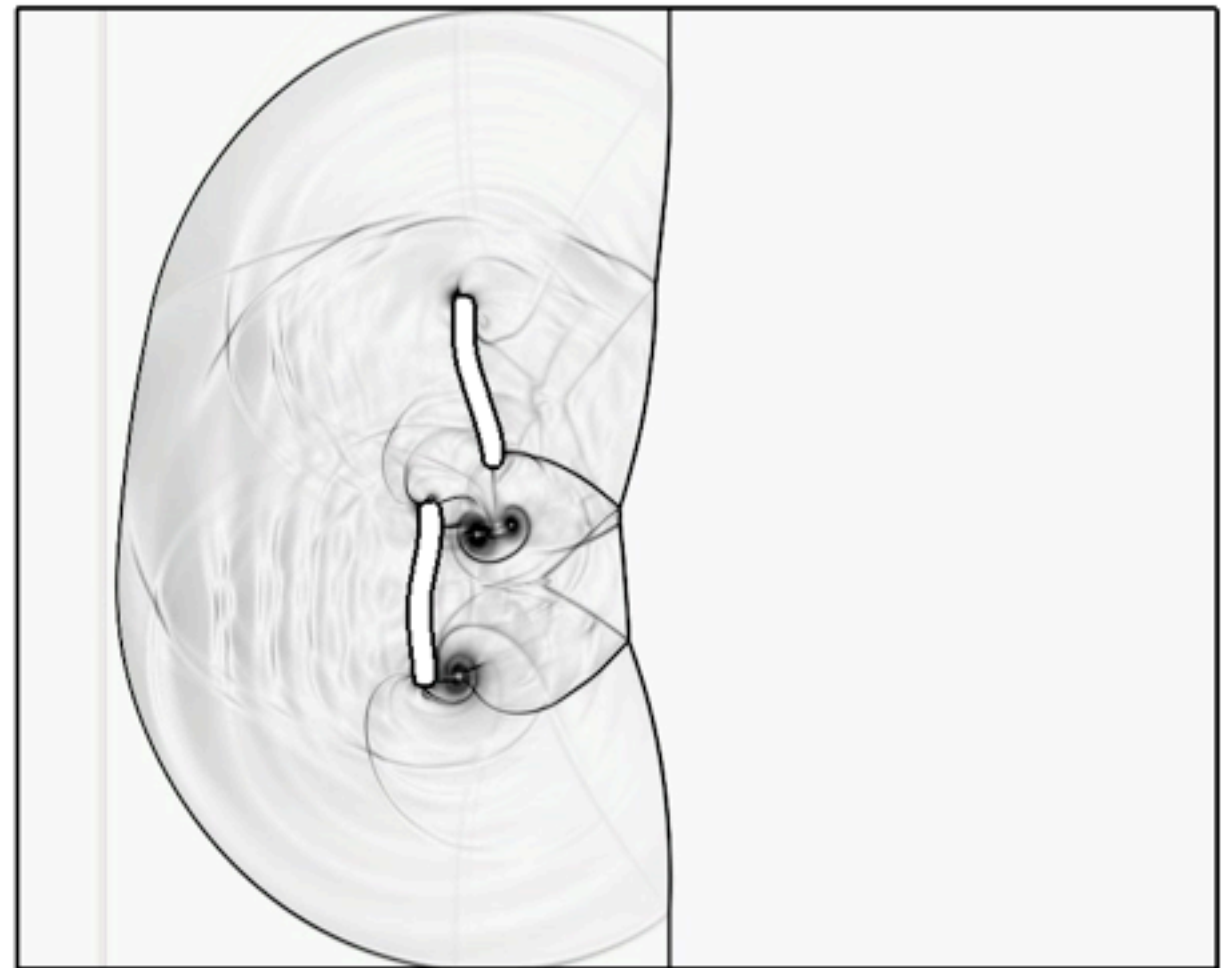
Example: Mach-2 shock impacting rigid sticks

Example: Mach-2 shock impacting
deformable sticks

In this work our target applications are high-speed compressible flows with embedded deforming or rigid solids

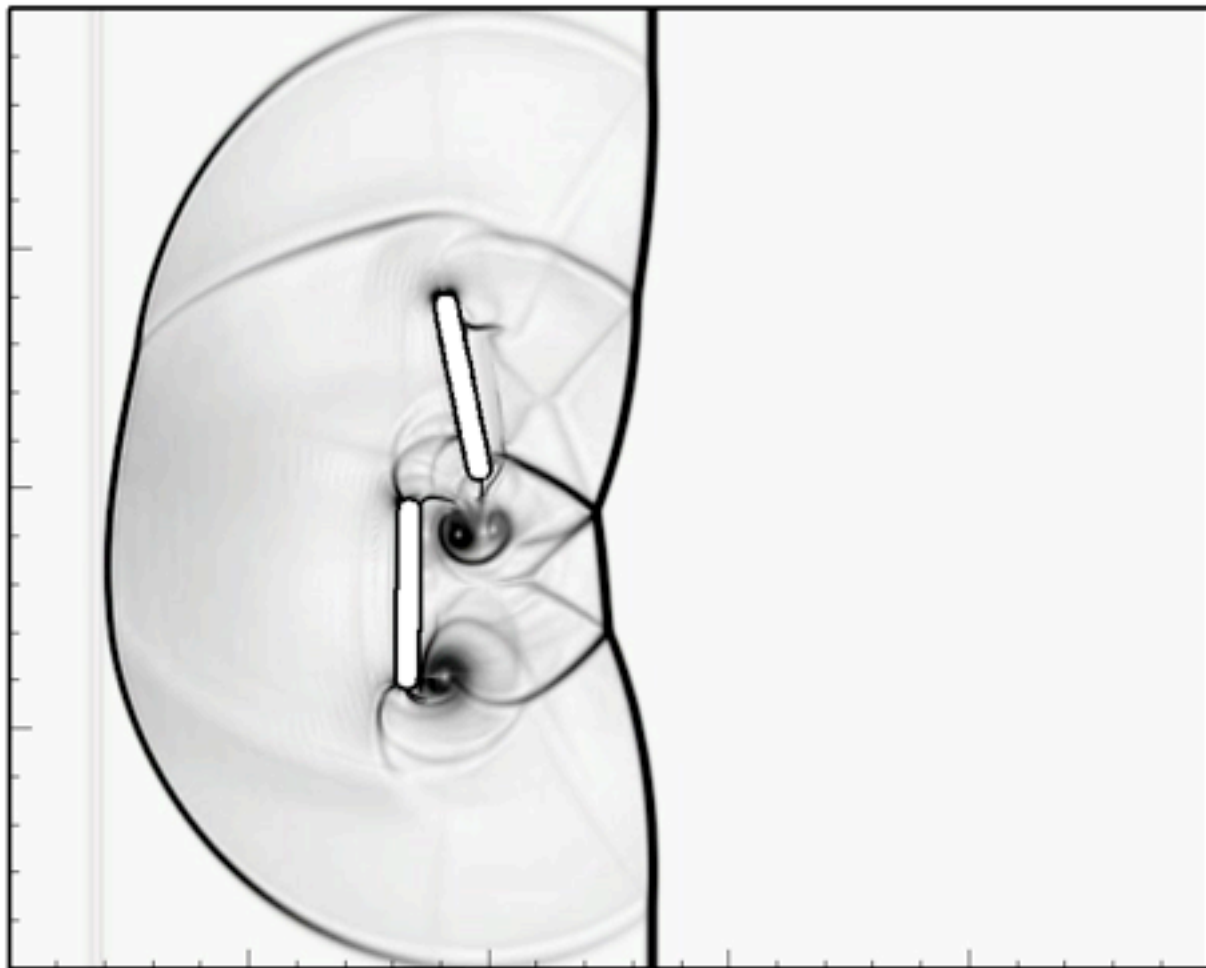


Example: Mach-2 shock impacting rigid sticks

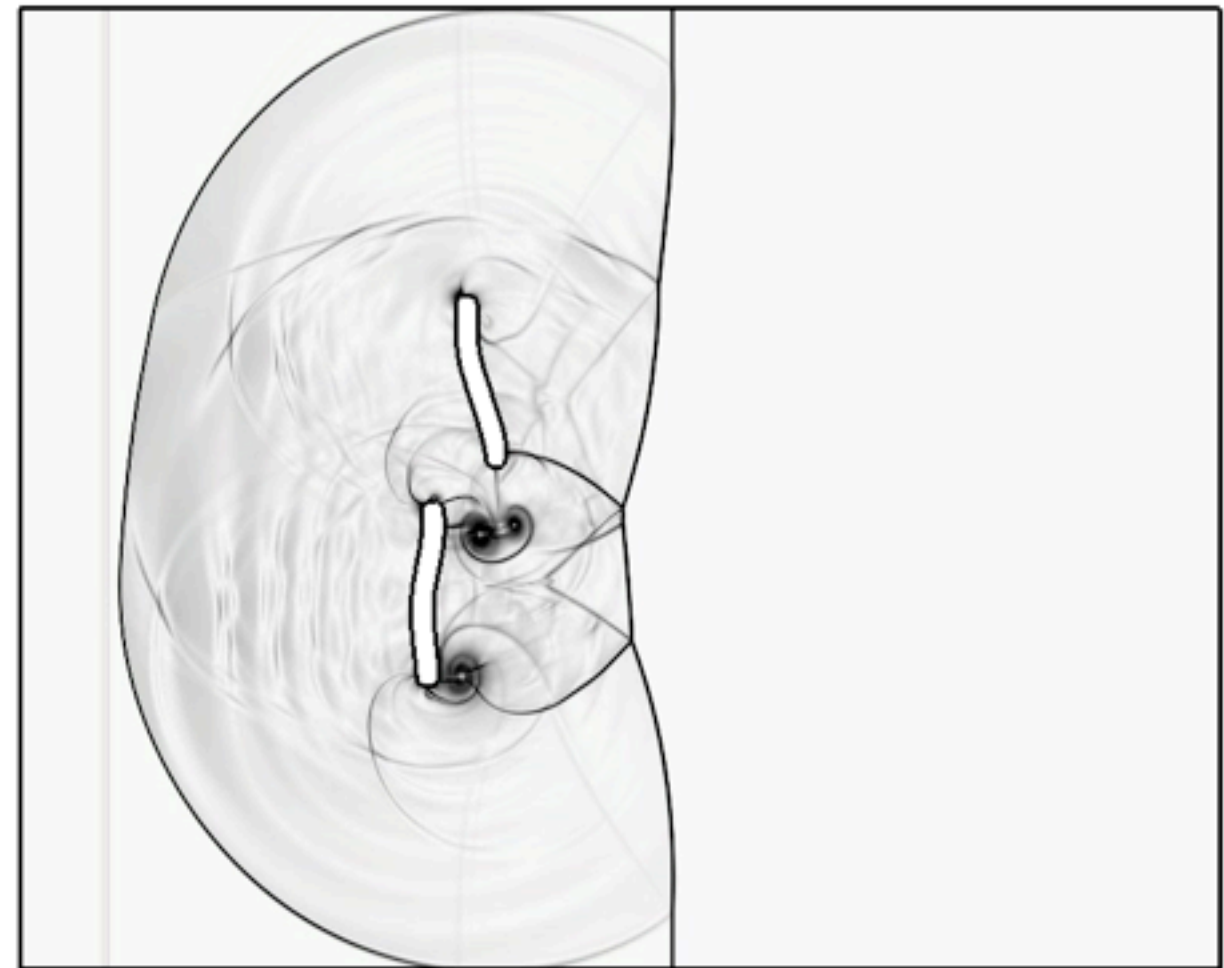


Example: Mach-2 shock impacting deformable sticks

In this work our target applications are high-speed compressible flows with embedded deforming or rigid solids



Example: Mach-2 shock impacting rigid sticks



Example: Mach-2 shock impacting deformable sticks

We are developing a new interface projection methodology to eliminate added mass instabilities in partitioned schemes

- Traditional partitioned FSI algorithms (Cirak, et. al. 2007, Bungartz and Schafer 2006)
 1. advance fluid (using interface velocity/position from the solid)
 2. advance solid (apply fluid forces to the solid)
- This approach suffers instability for light solids (added mass instability)
- Our new interface projection approach
 1. project solution at the interface
 2. advance fluid and solid
- Added mass instabilities can be avoided
- Stability is proved via. normal mode theory
- The analysis reveals very useful mathematical structure in FSI problems
- Added mass instabilities are discussed elsewhere in the literature, for example
 - Causin, Grebeau, and Nobile, 2005
 - Gretarsson, Kwatra, and Fedkiw 2011

We are developing a new interface projection methodology to eliminate added mass instabilities in partitioned schemes

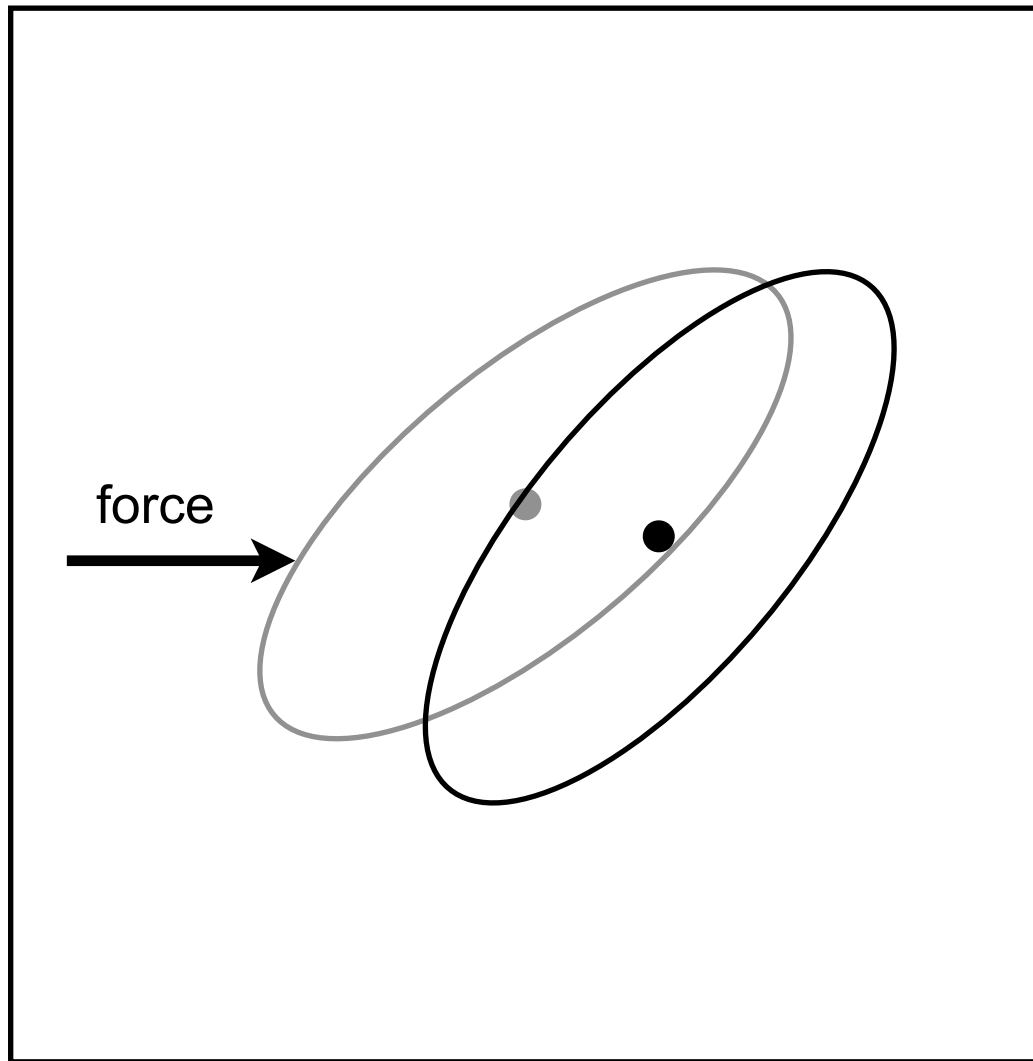
- Traditional partitioned FSI algorithms (Cirak, et. al. 2007, Bungartz and Schafer 2006)
 1. advance fluid (using interface velocity/position from the solid)
 2. advance solid (apply fluid forces to the solid)
- This approach suffers instability for light solids (added mass instability)
- Our new interface projection approach
 1. project solution at the interface
 2. advance fluid and solid
- Added mass instabilities can be avoided
- Stability is proved via. normal mode theory
- The analysis reveals very useful mathematical structure in FSI problems
- Added mass instabilities are discussed elsewhere in the literature, for example
 - Causin, Grebeau, and Nobile, 2005
 - Gretarsson, Kwatra, and Fedkiw 2011

We are developing a new interface projection methodology to eliminate added mass instabilities in partitioned schemes

- Traditional partitioned FSI algorithms (Cirak, et. al. 2007, Bungartz and Schafer 2006)
 1. advance fluid (using interface velocity/position from the solid)
 2. advance solid (apply fluid forces to the solid)
- This approach suffers instability for light solids (added mass instability)
- Our new interface projection approach
 1. project solution at the interface
 2. advance fluid and solid
- Added mass instabilities can be avoided
- Stability is proved via. normal mode theory
- The analysis reveals very useful mathematical structure in FSI problems
- Added mass instabilities are discussed elsewhere in the literature, for example
 - Causin, Grebeau, and Nobile, 2005
 - Gretarsson, Kwatra, and Fedkiw 2011

Added mass instabilities can arise if the effect of displaced fluid is not appropriately accounted for

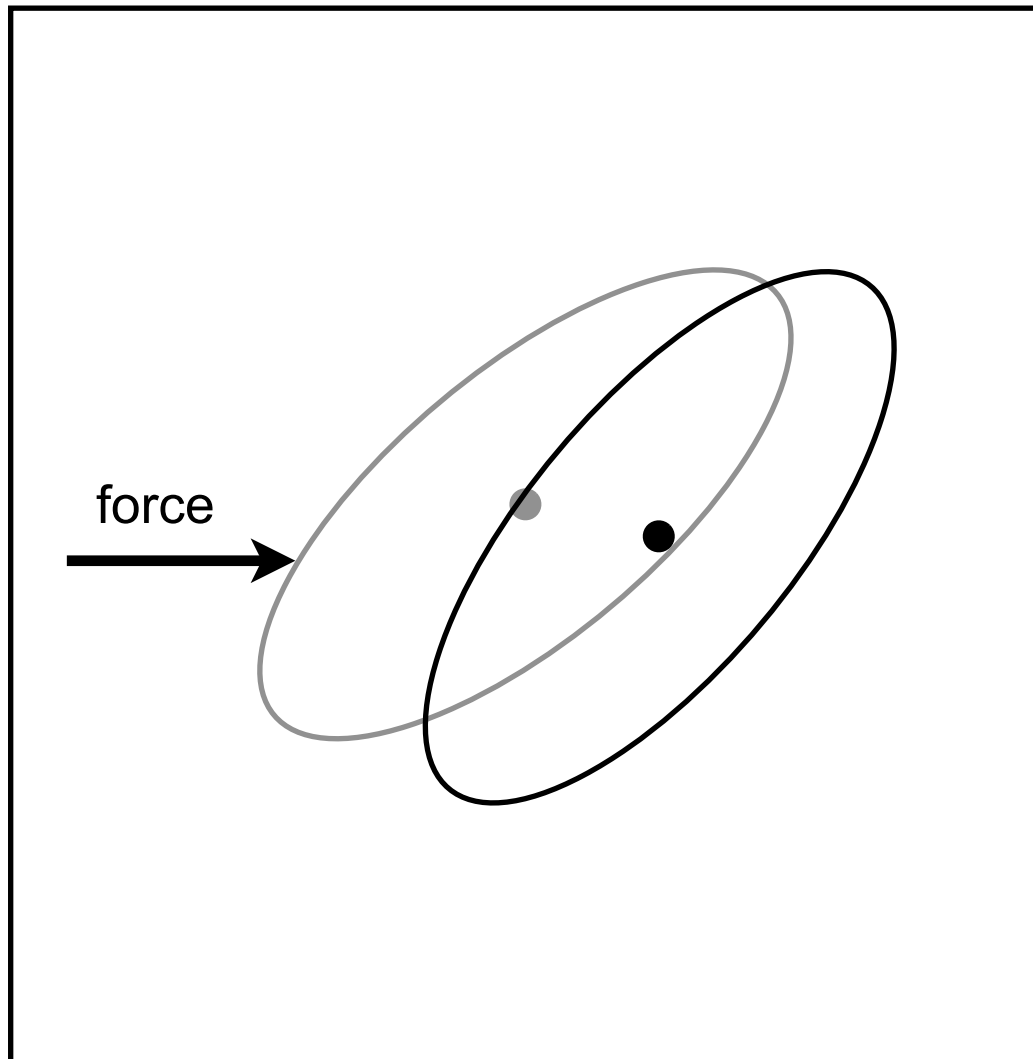
in a vacuum



Body simply moves according to
Newton's laws of motion

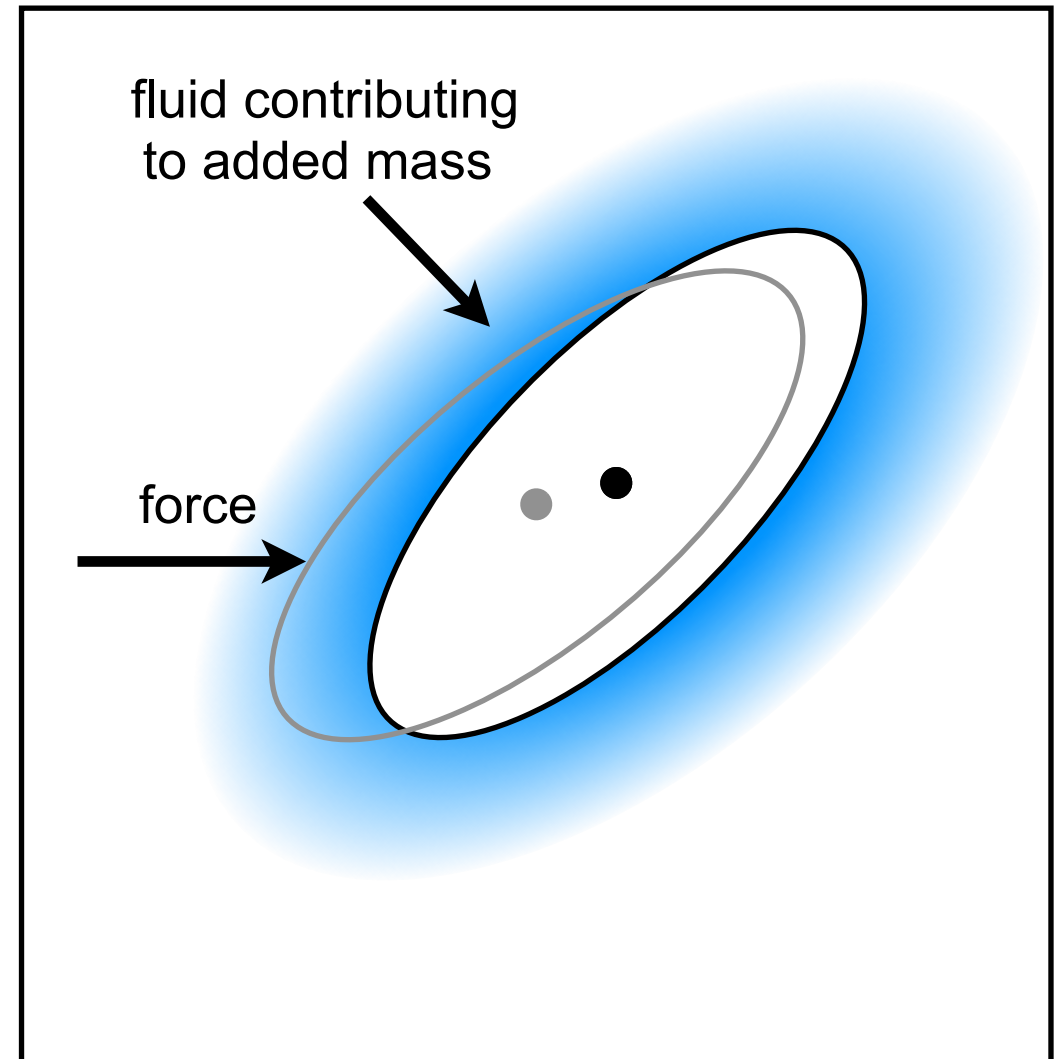
Added mass instabilities can arise if the effect of displaced fluid is not appropriately accounted for

in a vacuum



Body simply moves according to Newton's laws of motion

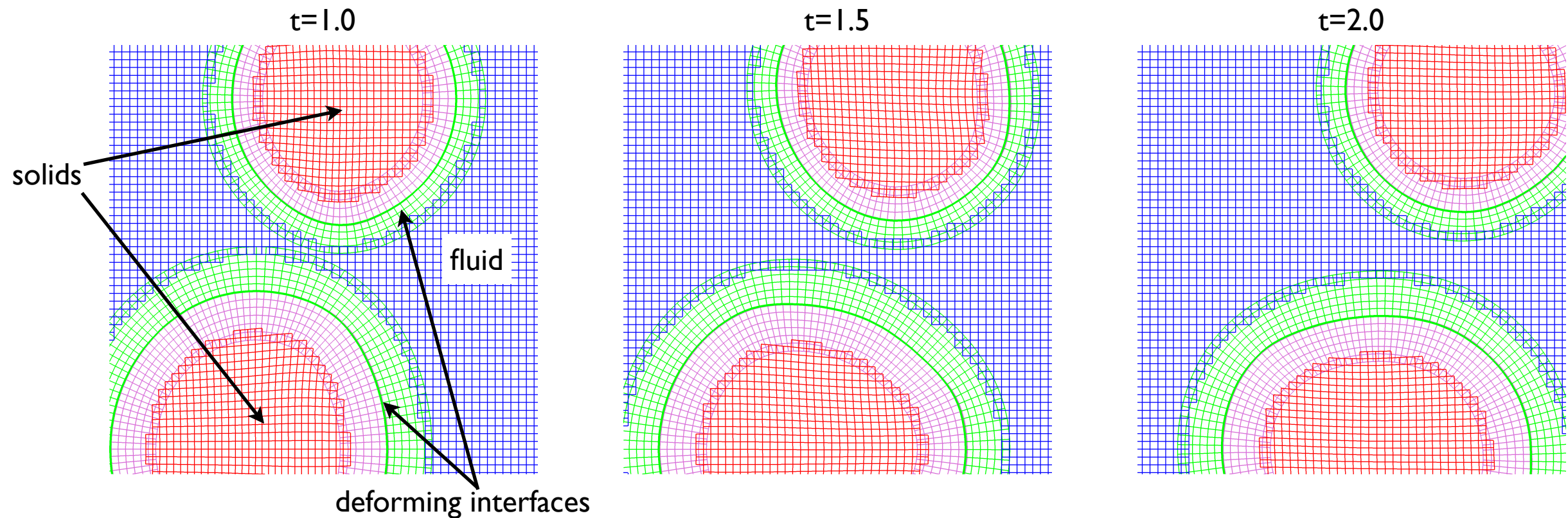
in a fluid



Body must displace and entrain fluid to move and therefore appears more massive than in vacuum ... the so called "added mass"

Deforming Composite Grids (DCGs) are an efficient way to discretize PDEs in deforming and/or moving geometry

- Overlapping grids are the foundation of DCGs



- Benefits of this approach include:
 - Local and rapid grid generation (hyperbolic grid generator)
 - High quality grids even under large displacements and rotations
 - High efficiency through the use of structured and Cartesian grids
 - Grid construction that supports high-order discretizations
- We use the Overture and CG software packages
 - www.llnl.gov/CASC/Overture

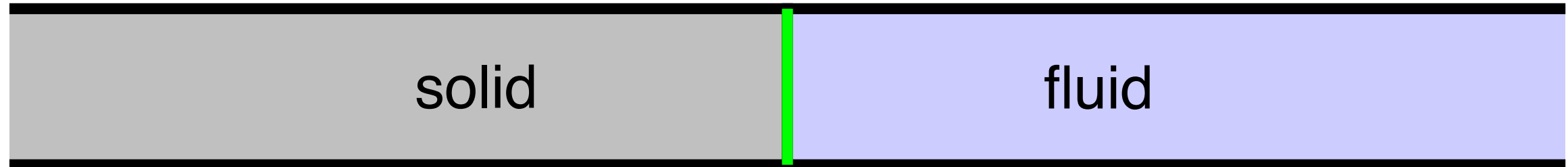
We pursue a partitioned approach for maximal efficiency and flexibility

- Fluid solver: we solve the inviscid Euler equations with a second-order extension of Godunov's method (cgcns)
 - WDH, D. W. Schwendeman, *Parallel Computation of Three-Dimensional Flows using Overlapping Grids with Adaptive Mesh Refinement*, J. Comput. Phys. **227** (2008)
 - WDH, D. W. Schwendeman, *An Adaptive Numerical Scheme for High-Speed Reactive Flow on Overlapping Grids*, J. Comput. Phys. **191** (2003)

- Solid solver: we solve the elastic wave equations as a first-order system with a second-order upwind scheme (cgsm)
 - D. Appelö, JWB, WDH, D. W. Schwendeman, *Numerical Methods for Solid Mechanics on Overlapping Grids: Linear Elasticity*, J. Comput. Phys. **231** (2012)

- Multidomain coupler: we use an interface projection scheme which is stable across the entire range of material parameters, including for light solids (cgmp)
 - JWB, WDH, B. Sjögren, *A stable FSI algorithm for light rigid bodies in compressible flows*, LLNL-JRNL-558232, submitted
 - B. Sjögren, JWB, *Stability of Finite Difference Discretizations of Multi-Physics Interface Conditions*, Commun. Comput. Phys., **13** (2013)
 - JWB, WDH, D. W. Schwendeman, *Deforming Composite Grids for Solving Fluid Structure Problems*, J. Comput. Phys. **231** (2012)
 - JWB, B. Sjögren, *A normal mode stability analysis of numerical interface conditions for fluid-structure interaction*, Commun. Comput. Phys., **10** (2011)

Greengard's Axiom: "It never hurts to start my writing down the exact solution to the problem"



Linear Elasticity

$$\begin{cases} \partial_t \bar{u} - \bar{v} = 0 \\ \bar{\rho} \partial_t \bar{v} - \partial_{\bar{x}} \bar{\sigma} = 0 \\ \partial_t \bar{\sigma} - \bar{\rho} c_p^2 \partial_{\bar{x}} \bar{v} = 0 \end{cases}$$

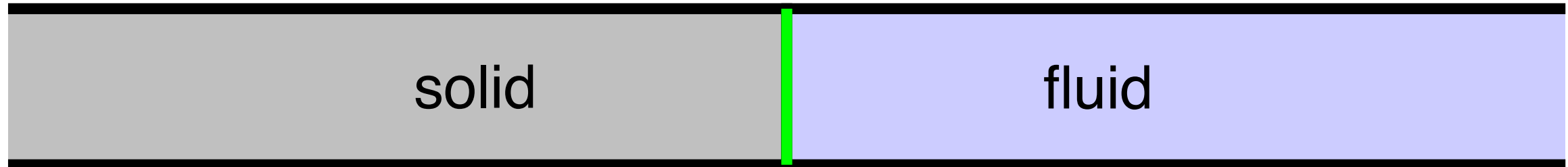
Euler Equations

$$\begin{cases} \partial_t \rho + \partial_x (\rho v) = 0 \\ \partial_t (\rho v) + \partial_x (\rho v^2 + p) = 0 \\ \partial_t (\rho E) + \partial_x (\rho E v + p v) = 0 \end{cases}$$

Interface Coupling Conditions

$$\begin{cases} \bar{v}(\bar{x}, t) = v(x, t), \\ \bar{\sigma}(\bar{x}, t) = \sigma(x, t) \equiv -p(x, t) + p_e \end{cases}$$

Greengard's Axiom: "It never hurts to start my writing down the exact solution to the problem"



Linear Elasticity

$$\begin{cases} \partial_t \bar{u} - \bar{v} = 0 \\ \bar{\rho} \partial_t \bar{v} - \partial_{\bar{x}} \bar{\sigma} = 0 \\ \partial_t \bar{\sigma} - \bar{\rho} c_p^2 \partial_{\bar{x}} \bar{v} = 0 \end{cases}$$

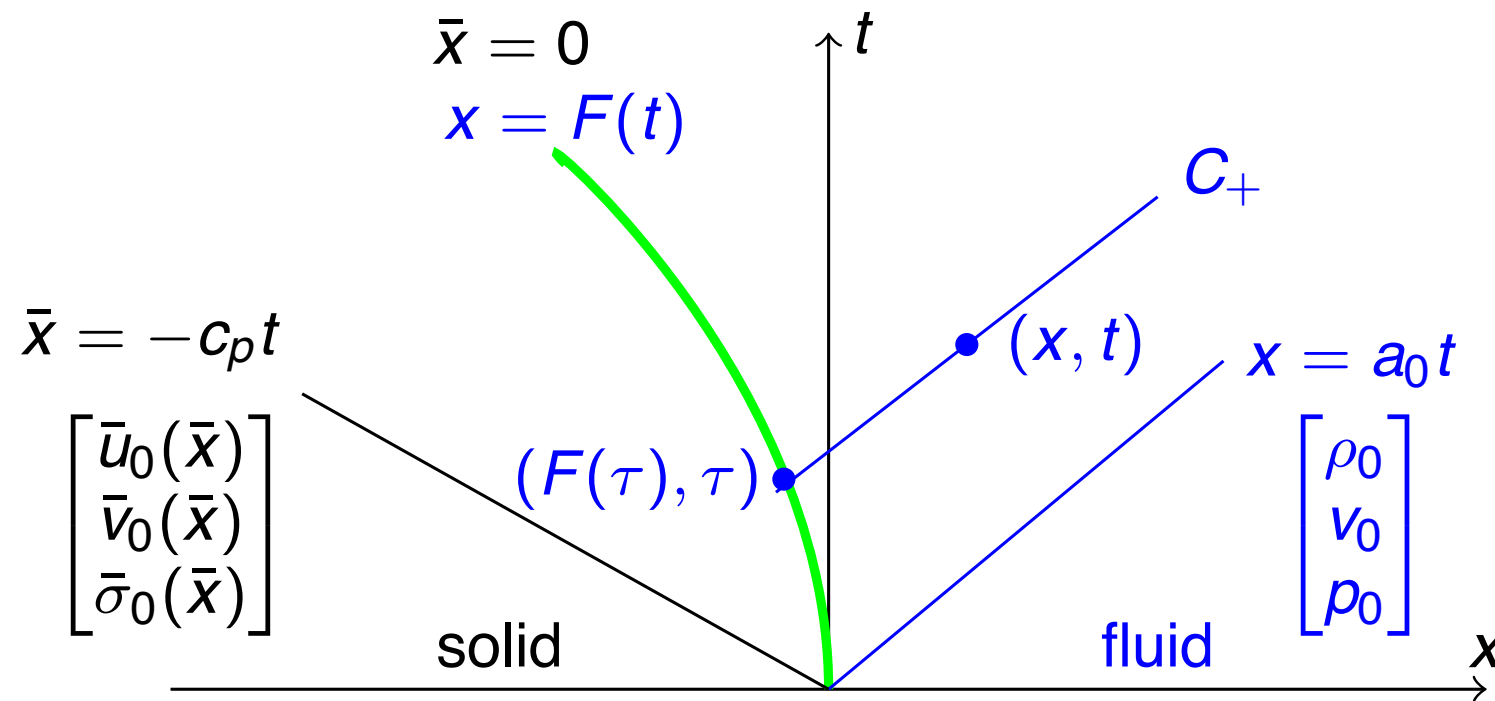
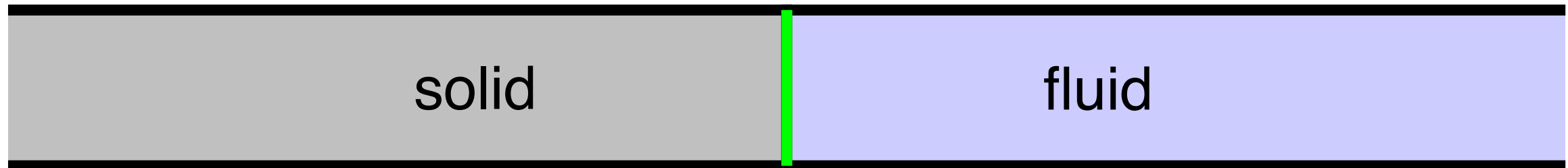
Euler Equations

$$\begin{cases} \partial_t \rho + \partial_x (\rho v) = 0 \\ \partial_t (\rho v) + \partial_x (\rho v^2 + p) = 0 \\ \partial_t (\rho E) + \partial_x (\rho E v + p v) = 0 \end{cases}$$

Interface Coupling Conditions

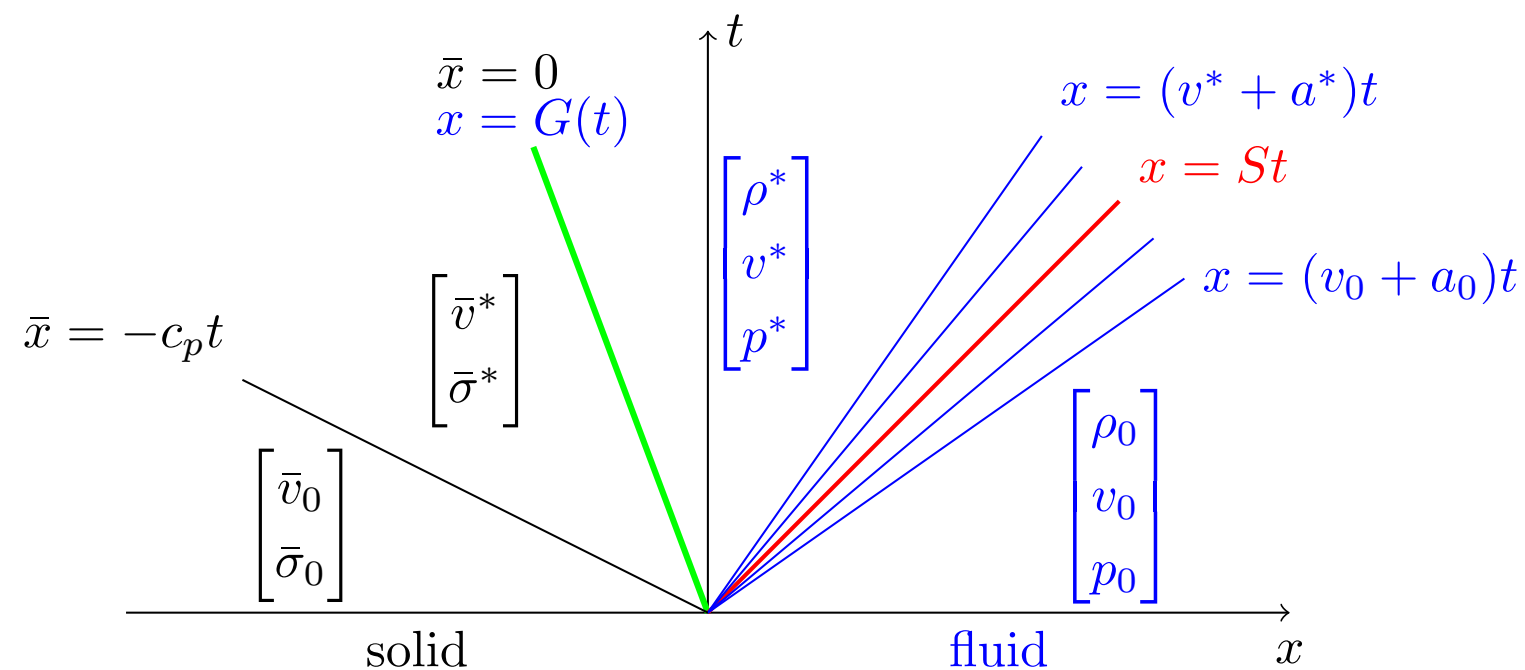
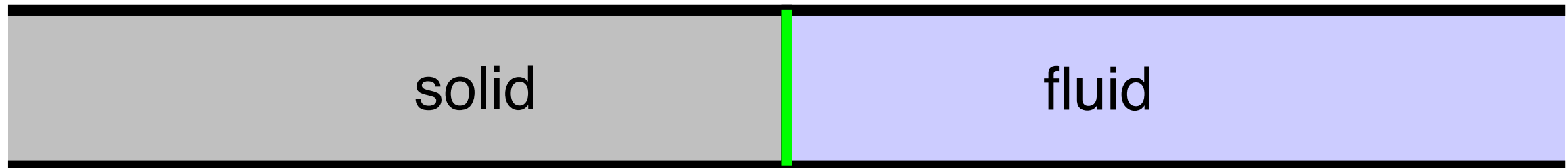
$$\begin{cases} \bar{v}(\bar{x}, t) = v(x, t), \\ \bar{\sigma}(\bar{x}, t) = \sigma(x, t) \equiv -p(x, t) + p_e \end{cases}$$

Greengard's Axiom: "It never hurts to start my writing down the exact solution to the problem"



- We call this the "elastic piston" problem

By localizing the elastic piston problem we obtain a fluid structure Riemann problem (FSRP) that can be used for FSI coupling



- This is a specific case of the elastic piston problem
 - Constant states in fluid and solid
- Exact solutions to the linear and nonlinear problem are easily found

The solution at the interface is defined in terms of solutions to the FSRP

- Along the interface, the solution is projected using solutions to local FSRPs

$$v_I = \frac{\bar{z}\bar{v}_0 + zv_0}{\bar{z} + z} + \frac{\sigma_0 - \bar{\sigma}_0}{\bar{z} + z}$$
$$\sigma_I = \frac{\bar{z}^{-1}\bar{\sigma}_0 + z^{-1}\sigma_0}{\bar{z}^{-1} + z^{-1}} + \frac{v_0 - \bar{v}_0}{\bar{z}^{-1} + z^{-1}}$$
$$\rho_I = \rho_0(p_I/p_0)^{1/\gamma}$$

- The traditional FSI coupling is the large impedance (mass) limit $\bar{z} \gg z$
 - velocity from solid $v_I = \bar{v}_0$
 - stress from fluid $\sigma_I = \sigma_0 = -p_0 + p_e$
- The traditional scheme is unstable for light solids
- The new scheme is stable for any ratio of masses and impedances
- For proofs see JWB, B. Sjögreen, *A normal mode stability analysis of numerical interface conditions for fluid-structure interaction*, Commun. Comput. Phys., **10** (2011)
- Here $\bar{z} = \bar{\rho}c_p$ and $z = \rho_0a_0$ are acoustic impedances

The solution at the interface is defined in terms of solutions to the FSRP

- Along the interface, the solution is projected using solutions to local FSRPs

$$v_I = \frac{\bar{z}\bar{v}_0 + zv_0}{\bar{z} + z} + \frac{\sigma_0 - \bar{\sigma}_0}{\bar{z} + z}$$
$$\sigma_I = \frac{\bar{z}^{-1}\bar{\sigma}_0 + z^{-1}\sigma_0}{\bar{z}^{-1} + z^{-1}} + \frac{v_0 - \bar{v}_0}{\bar{z}^{-1} + z^{-1}}$$
$$\rho_I = \rho_0(p_I/p_0)^{1/\gamma}$$

- The traditional FSI coupling is the large impedance (mass) limit $\bar{z} \gg z$
 - velocity from solid $v_I = \bar{v}_0$
 - stress from fluid $\sigma_I = \sigma_0 = -p_0 + p_e$
- The traditional scheme is unstable for light solids
- The new scheme is stable for any ratio of masses and impedances
- For proofs see JWB, B. Sjögreen, *A normal mode stability analysis of numerical interface conditions for fluid-structure interaction*, Commun. Comput. Phys., **10** (2011)
- Here $\bar{z} = \bar{\rho}c_p$ and $z = \rho_0a_0$ are acoustic impedances

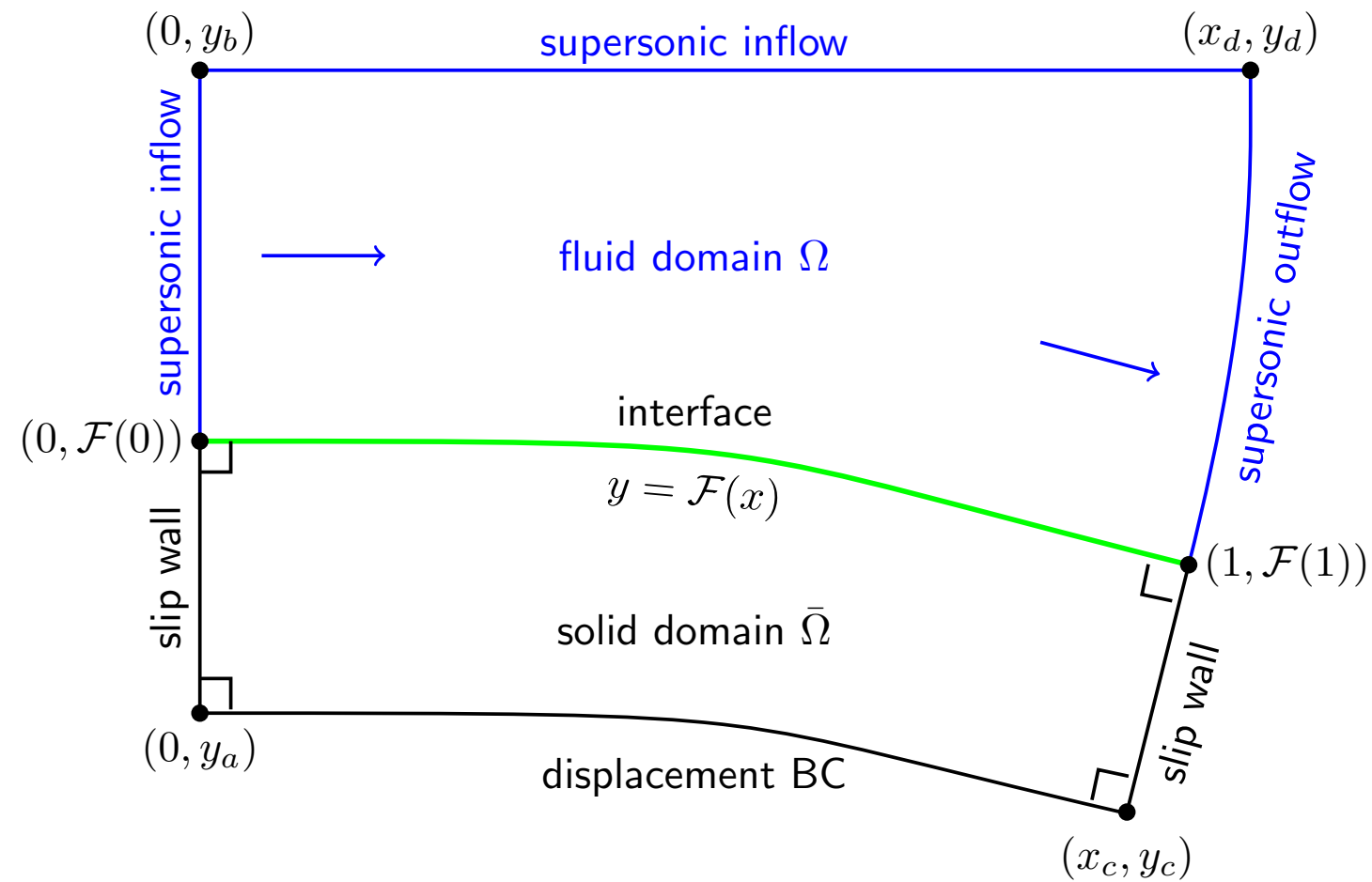
The solution at the interface is defined in terms of solutions to the FSRP

- Along the interface, the solution is projected using solutions to local FSRPs

$$v_I = \frac{\bar{z}\bar{v}_0 + zv_0}{\bar{z} + z} + \frac{\sigma_0 - \bar{\sigma}_0}{\bar{z} + z}$$
$$\sigma_I = \frac{\bar{z}^{-1}\bar{\sigma}_0 + z^{-1}\sigma_0}{\bar{z}^{-1} + z^{-1}} + \frac{v_0 - \bar{v}_0}{\bar{z}^{-1} + z^{-1}}$$
$$\rho_I = \rho_0(p_I/p_0)^{1/\gamma}$$

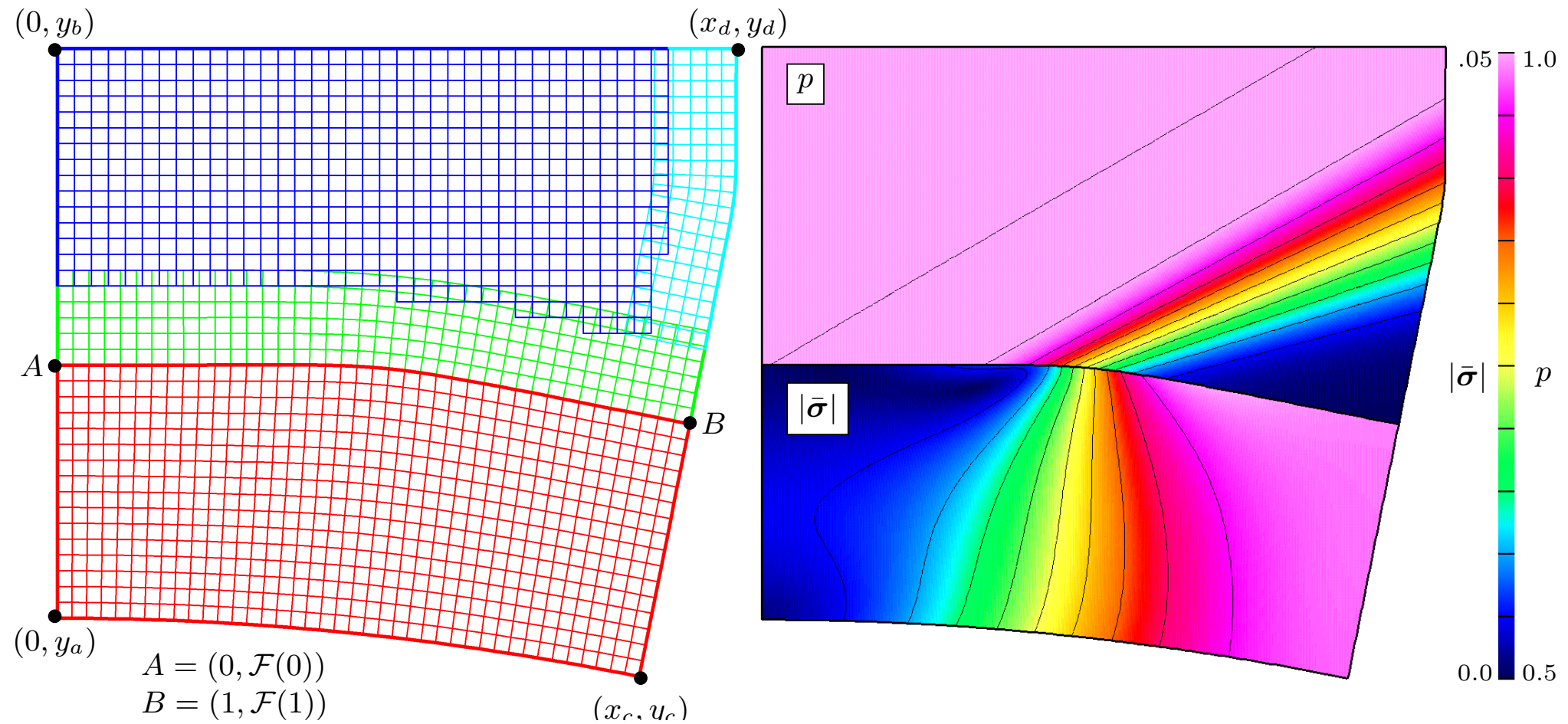
- The traditional FSI coupling is the large impedance (mass) limit $\bar{z} \gg z$
 - velocity from solid $v_I = \bar{v}_0$
 - stress from fluid $\sigma_I = \sigma_0 = -p_0 + p_e$
- The traditional scheme is unstable for light solids
- The new scheme is stable for any ratio of masses and impedances
- For proofs see JWB, B. Sjögreen, *A normal mode stability analysis of numerical interface conditions for fluid-structure interaction*, Commun. Comput. Phys., **10** (2011)
- Here $\bar{z} = \bar{\rho}c_p$ and $z = \rho_0a_0$ are acoustic impedances

The deforming diffuser solution can be used to investigate convergence in 2D



- A coupled semi-analytic smooth solution is determined:
 - Fluid: Prandtl-Meyer analytic solution as a function of $F(x)$
 - Solid: steady elasticity equations are solved on a very fine grid
 - The coupled exact solution and $F(x)$ are determined by iteration

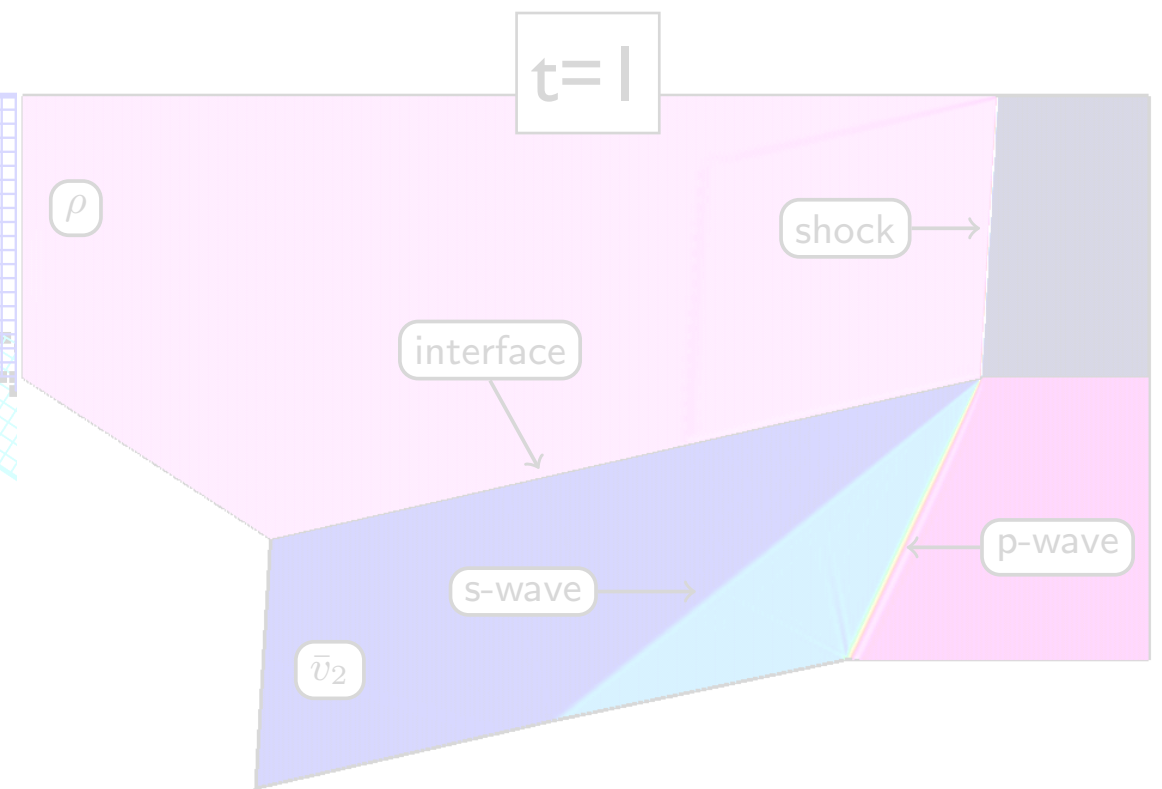
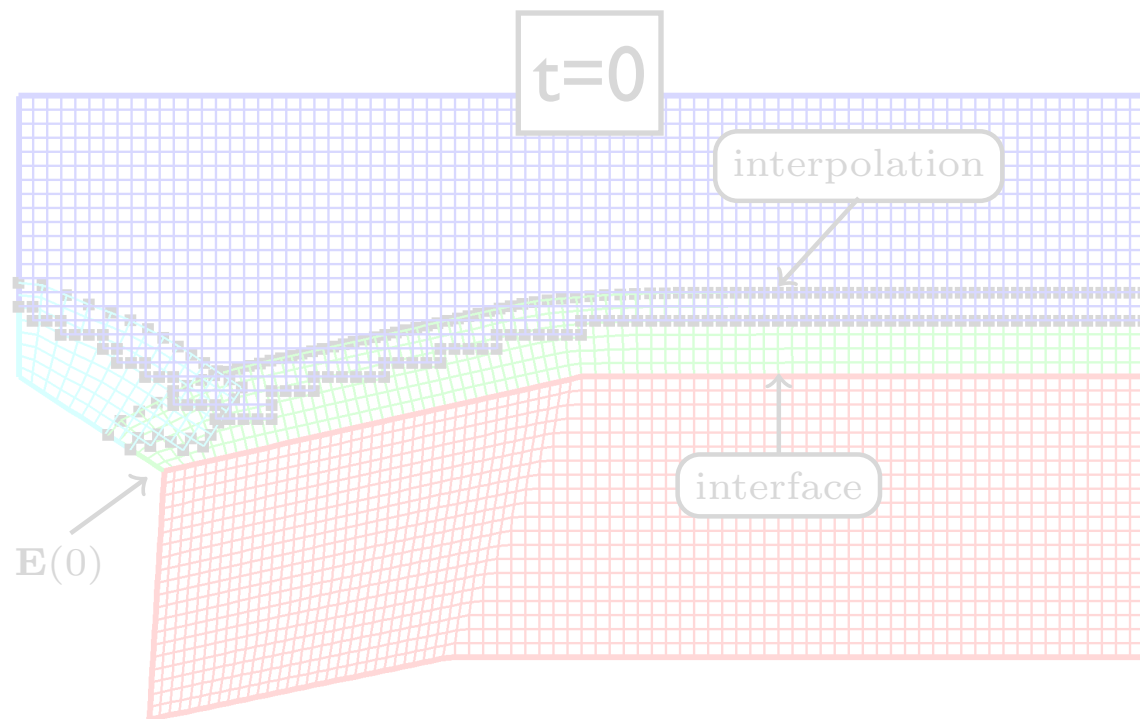
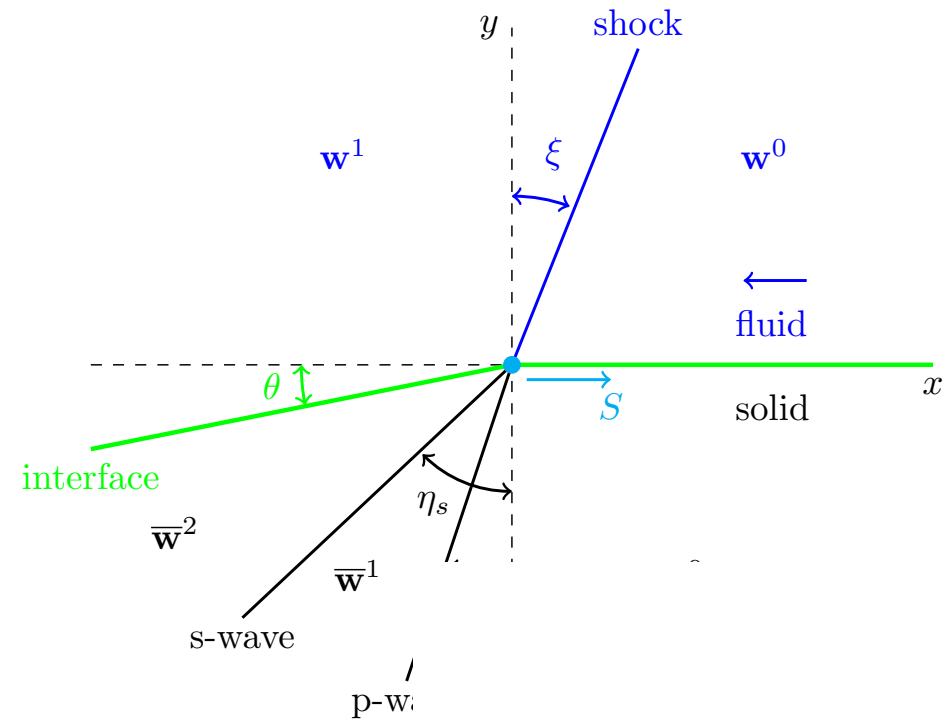
The deforming diffuser solution can be used to investigate convergence in 2D



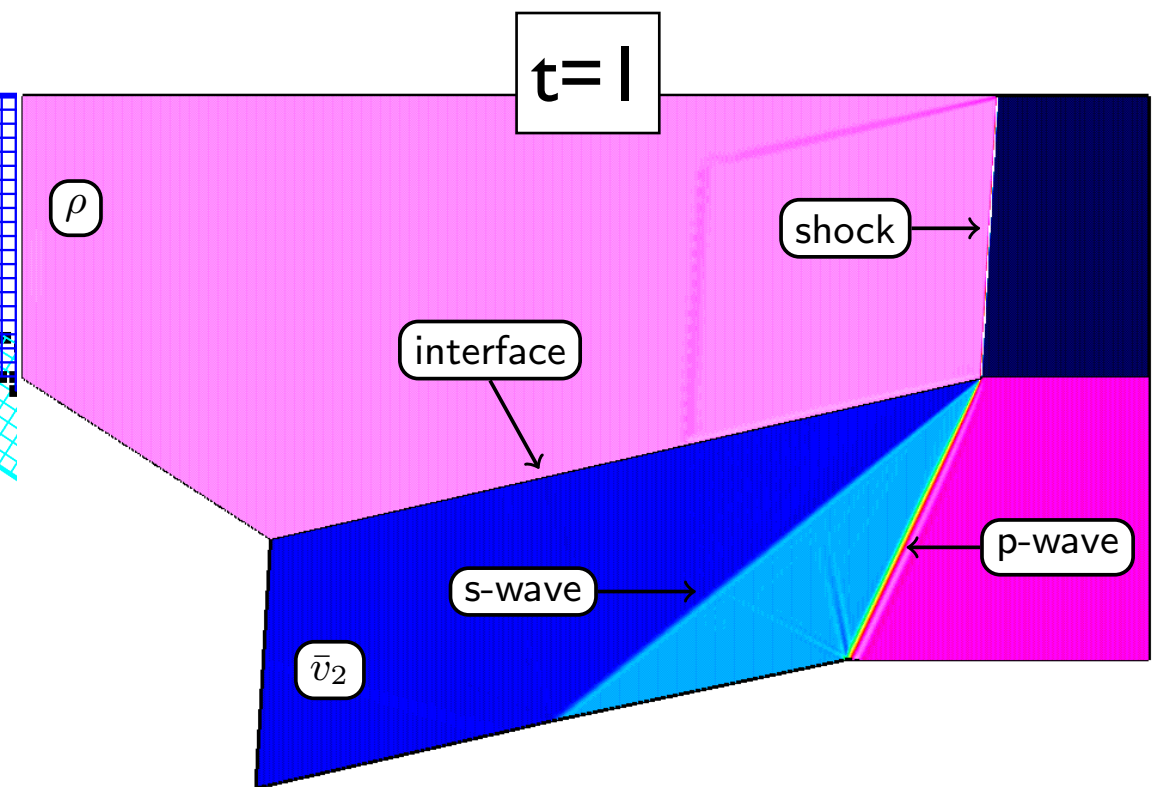
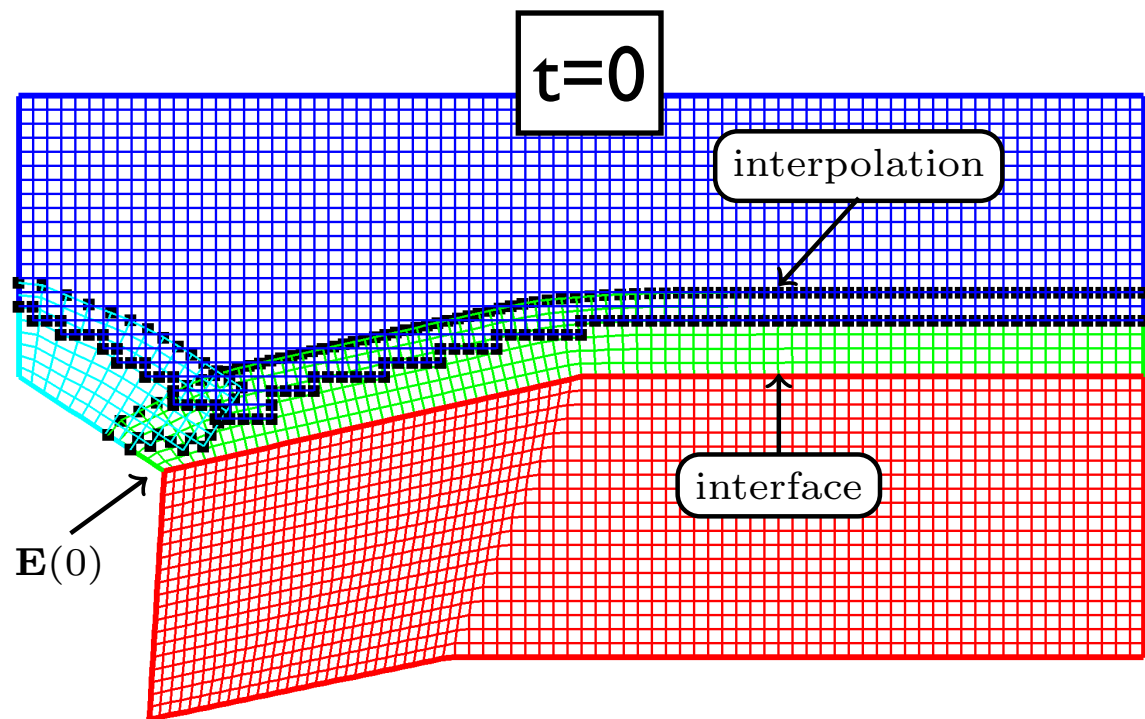
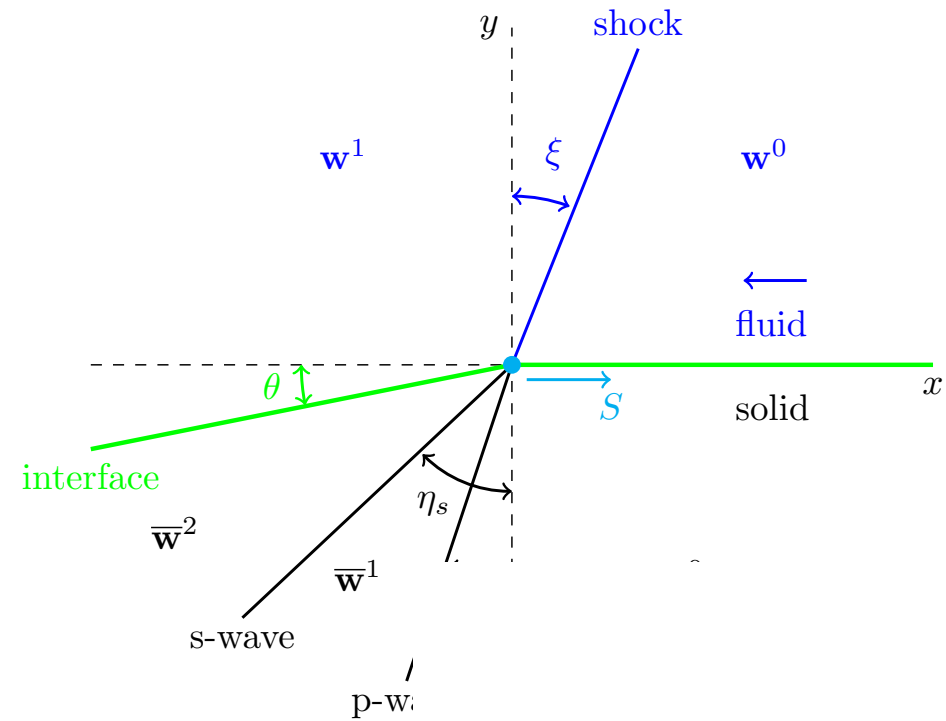
Grid	Solid						Fluid					
	$\mathcal{E}_{\bar{\mathbf{u}}}^{(\infty)}$	r	$\mathcal{E}_{\bar{\mathbf{v}}}^{(\infty)}$	r	$\mathcal{E}_{\bar{\sigma}}^{(\infty)}$	r	$\mathcal{E}_{\rho}^{(\infty)}$	r	$\mathcal{E}_{\mathbf{v}}^{(\infty)}$	r	$\mathcal{E}_T^{(\infty)}$	r
$\mathcal{G}_{dd}^{(2)}$	1.6e-4		2.8e-4		2.9e-2		3.4e-2		2.1e-2		7.0e-3	
$\mathcal{G}_{dd}^{(4)}$	3.3e-5	4.8	1.1e-4	2.6	8.9e-3	3.3	8.6e-3	3.9	6.3e-3	3.4	1.9e-3	3.8
$\mathcal{G}_{dd}^{(8)}$	5.6e-6	5.9	2.8e-5	3.9	1.8e-3	5.0	2.2e-3	3.8	2.1e-3	3.0	5.9e-4	3.2
$\mathcal{G}_{dd}^{(16)}$	9.4e-7	5.9	6.8e-6	4.1	3.5e-4	5.0	5.8e-4	3.8	4.7e-4	4.4	1.3e-4	4.4
rate	2.48		1.81		2.14		1.95		1.81		1.88	

- Max norm convergence verifies second-order accuracy

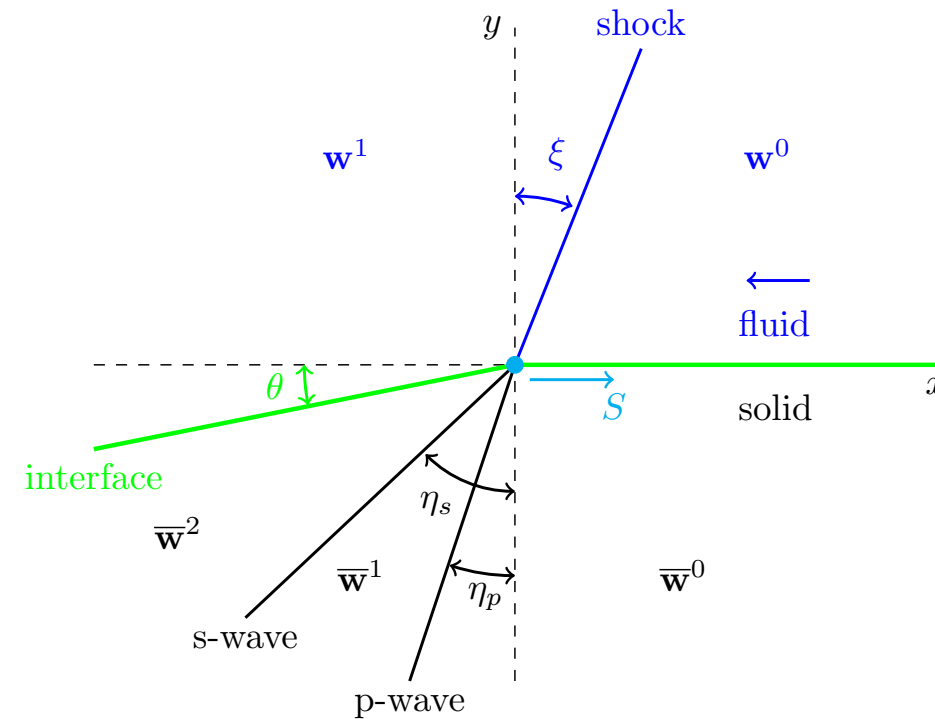
The superseismic shock problem is used to demonstrate convergence for problems with discontinuities



The superseismic shock problem is used to demonstrate convergence for problems with discontinuities



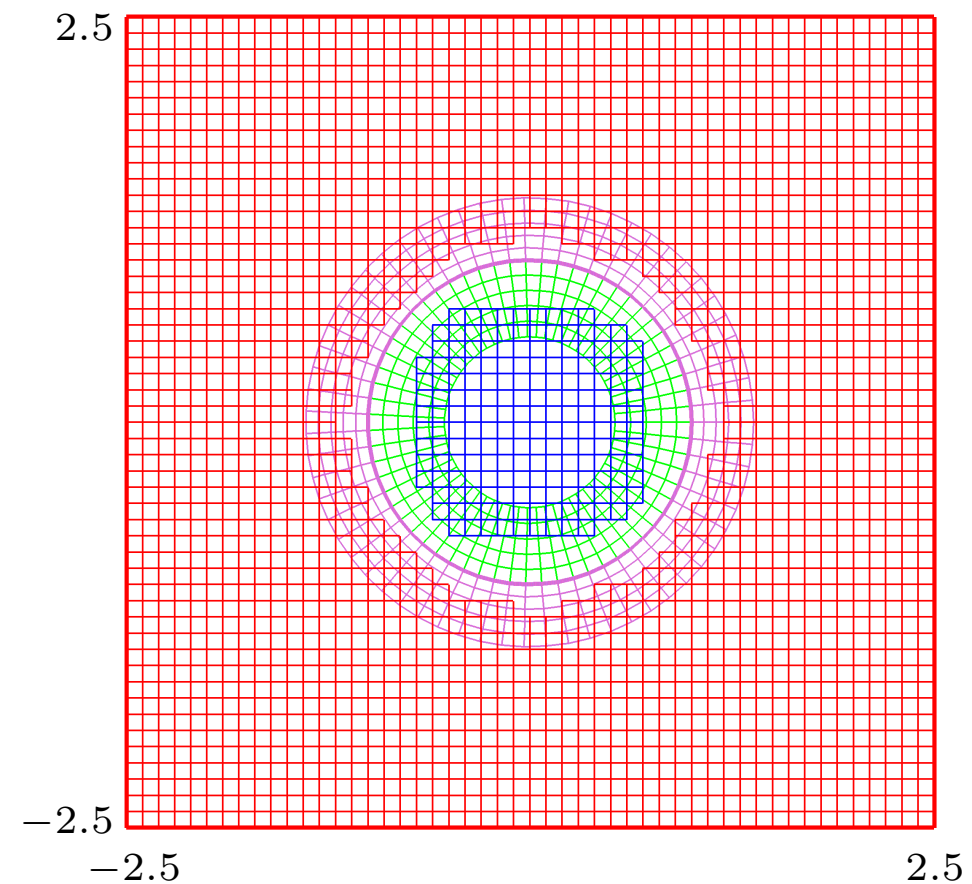
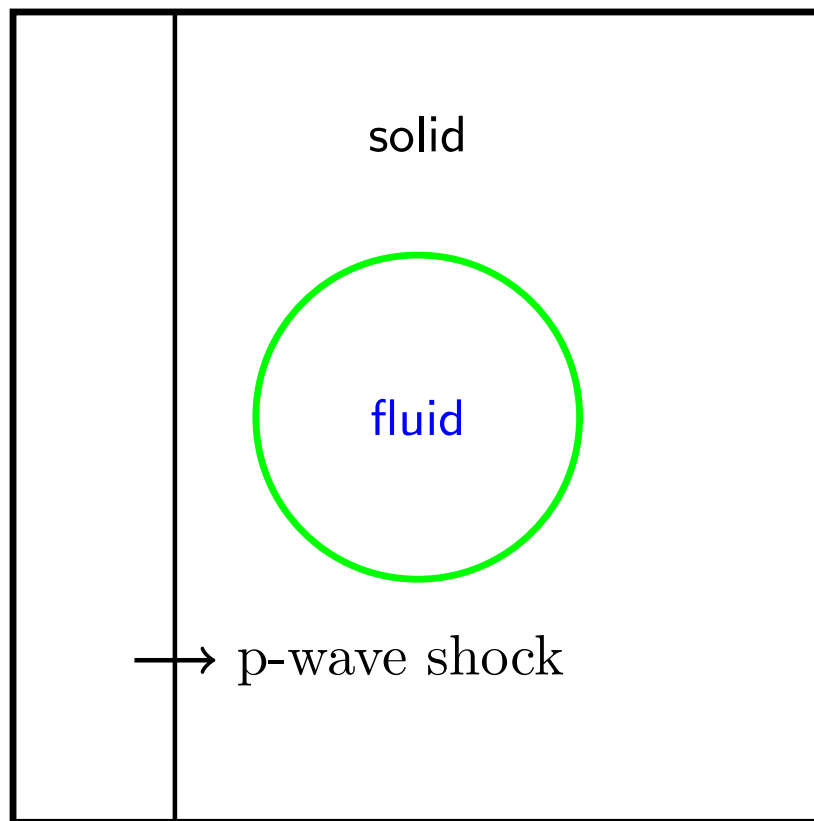
The superseismic shock problem is used to demonstrate convergence for problems with discontinuities



- L-1 norm convergence results demonstrate expected behavior

Grid	Solid						Fluid					
	$\mathcal{E}_{\bar{u}}^{(1)}$	r	$\mathcal{E}_{\bar{v}}^{(1)}$	r	$\mathcal{E}_{\bar{\sigma}}^{(1)}$	r	$\mathcal{E}_{\rho}^{(1)}$	r	$\mathcal{E}_{v}^{(1)}$	r	$\mathcal{E}_T^{(1)}$	r
$\mathcal{G}_{ss}^{(4)}$	8.9e-4		6.4e-3		1.8e-2		5.9e-3		3.8e-2		1.2e-2	
$\mathcal{G}_{ss}^{(8)}$	3.2e-4	2.8	3.9e-3	1.6	1.1e-2	1.6	2.9e-3	2.0	1.7e-2	2.2	6.7e-3	1.8
$\mathcal{G}_{ss}^{(16)}$	1.4e-4	2.4	2.4e-3	1.7	6.7e-3	1.7	1.6e-3	1.9	8.6e-3	2.0	3.7e-3	1.8
$\mathcal{G}_{ss}^{(32)}$	6.7e-5	2.0	1.4e-3	1.6	4.1e-3	1.6	8.2e-4	1.9	4.3e-3	2.0	1.9e-3	1.9
rate	1.24		0.72		0.72		0.94		1.03		0.88	

Self-convergence is measured for a difficult problem of a fluid cylinder impacted by a solid compression wave

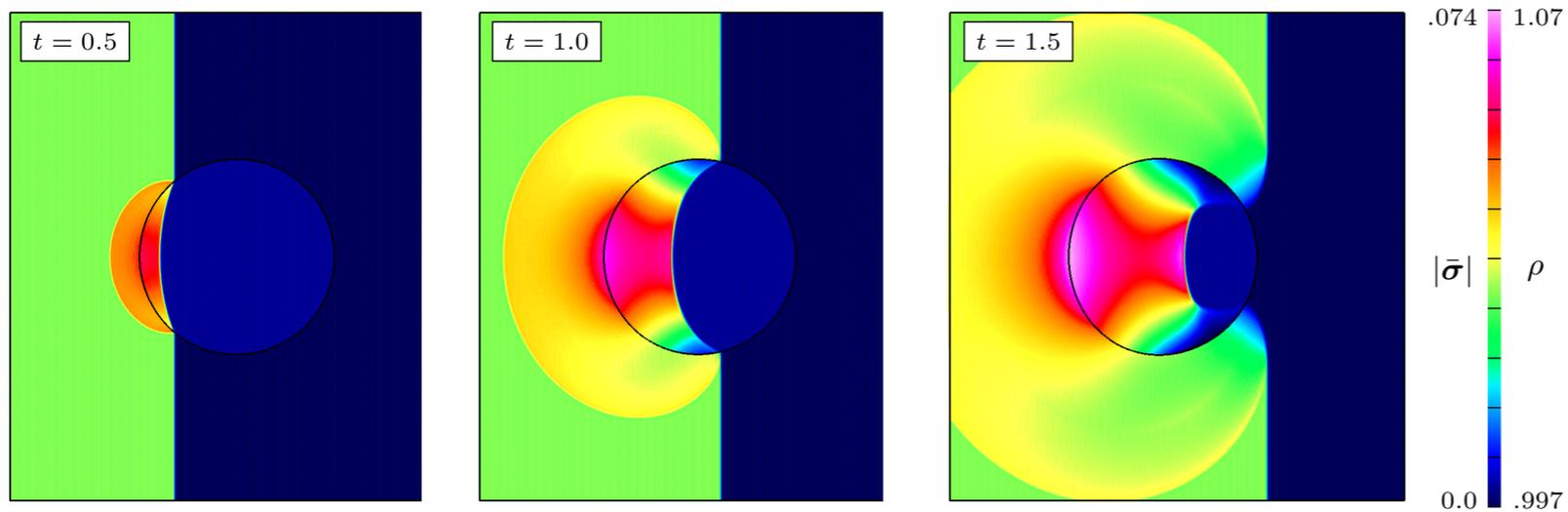


- L-1 norm convergence results demonstrate expected behavior

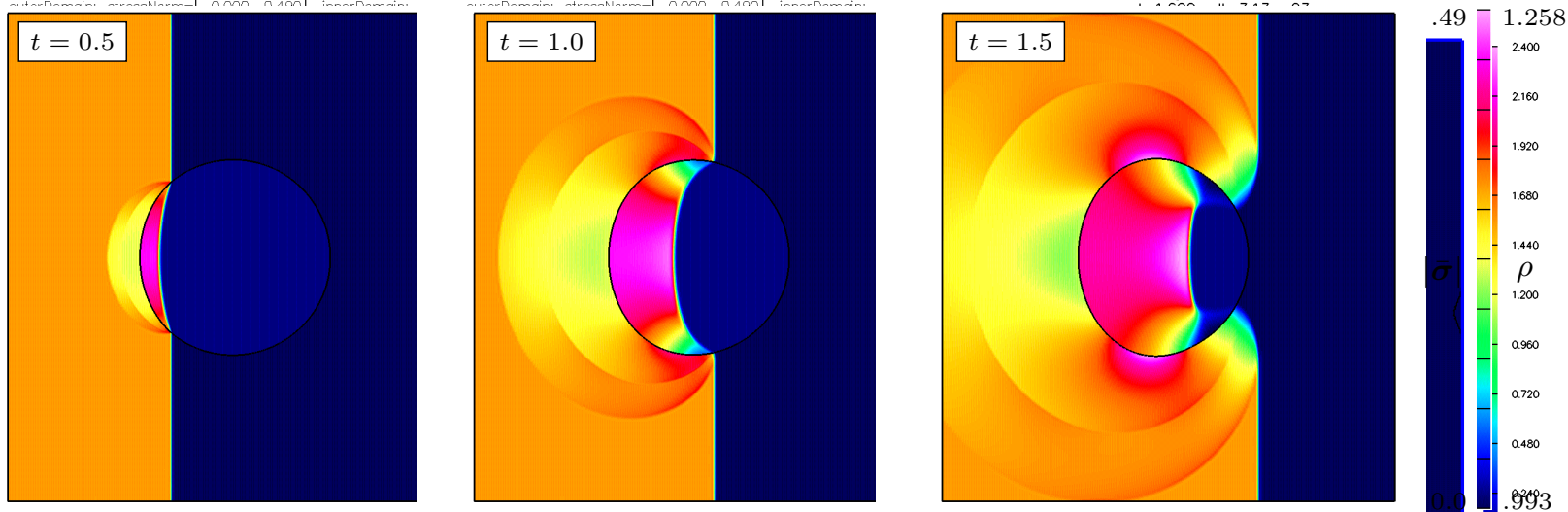
Grid	Solid						Fluid					
	$\mathcal{E}_{\bar{\mathbf{u}}}^{(1)}$	r	$\mathcal{E}_{\bar{\mathbf{v}}}^{(1)}$	r	$\mathcal{E}_{\bar{\sigma}}^{(1)}$	r	$\mathcal{E}_{\rho}^{(1)}$	r	$\mathcal{E}_{\mathbf{v}}^{(1)}$	r	$\mathcal{E}_T^{(1)}$	r
$\mathcal{G}_{dc}^{(4)}$	1.7e-4		1.1e-3		1.3e-3		4.1e-3		2.3e-3		4.2e-3	
$\mathcal{G}_{dc}^{(8)}$	7.9e-5	2.1	6.9e-4	1.6	7.9e-4	1.6	2.2e-3	1.8	1.3e-3	1.8	2.3e-3	1.8
$\mathcal{G}_{dc}^{(64)}$	8.3e-6	9.5	1.5e-4	4.5	1.8e-4	4.3	3.6e-4	6.3	2.1e-4	6.1	3.7e-4	6.2
rate	1.08		0.72		0.71		0.88		0.87		0.88	

Stability of partitioned solver for a variety of fluid/solid densities is demonstrated

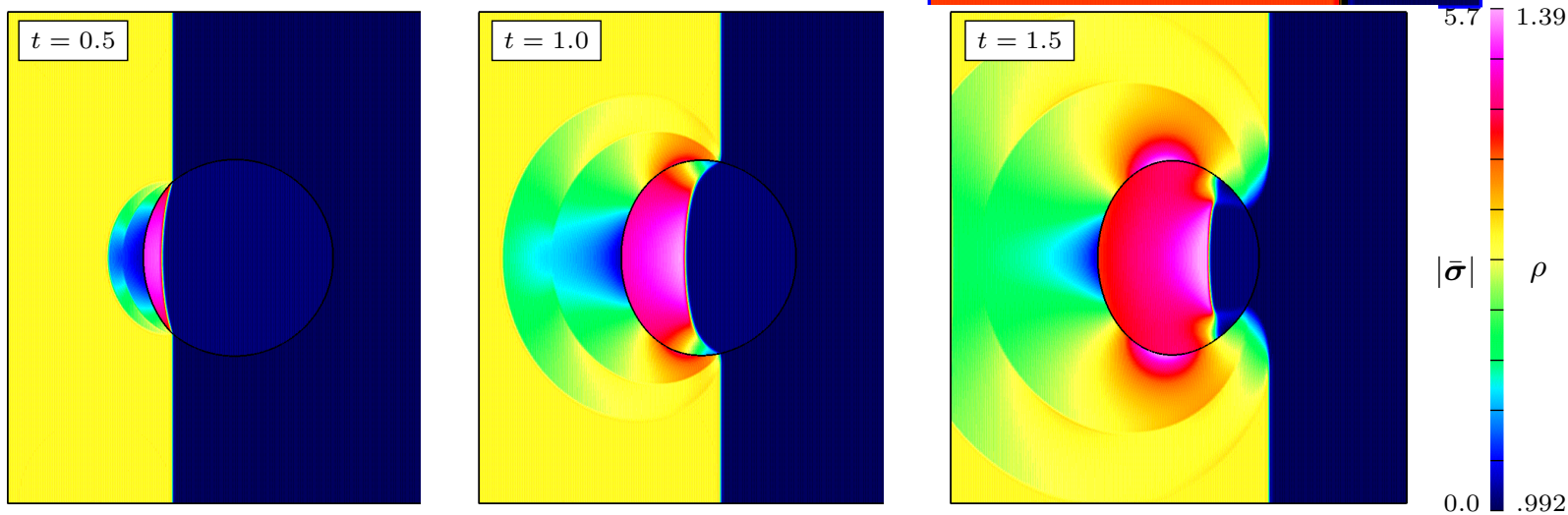
(example of solid compression wave impacting fluid cavity)



light solid
 $\bar{\rho} = 0.1$
Traditional coupling fails!



medium solid
 $\bar{\rho} = 1.0$
Traditional coupling fails!



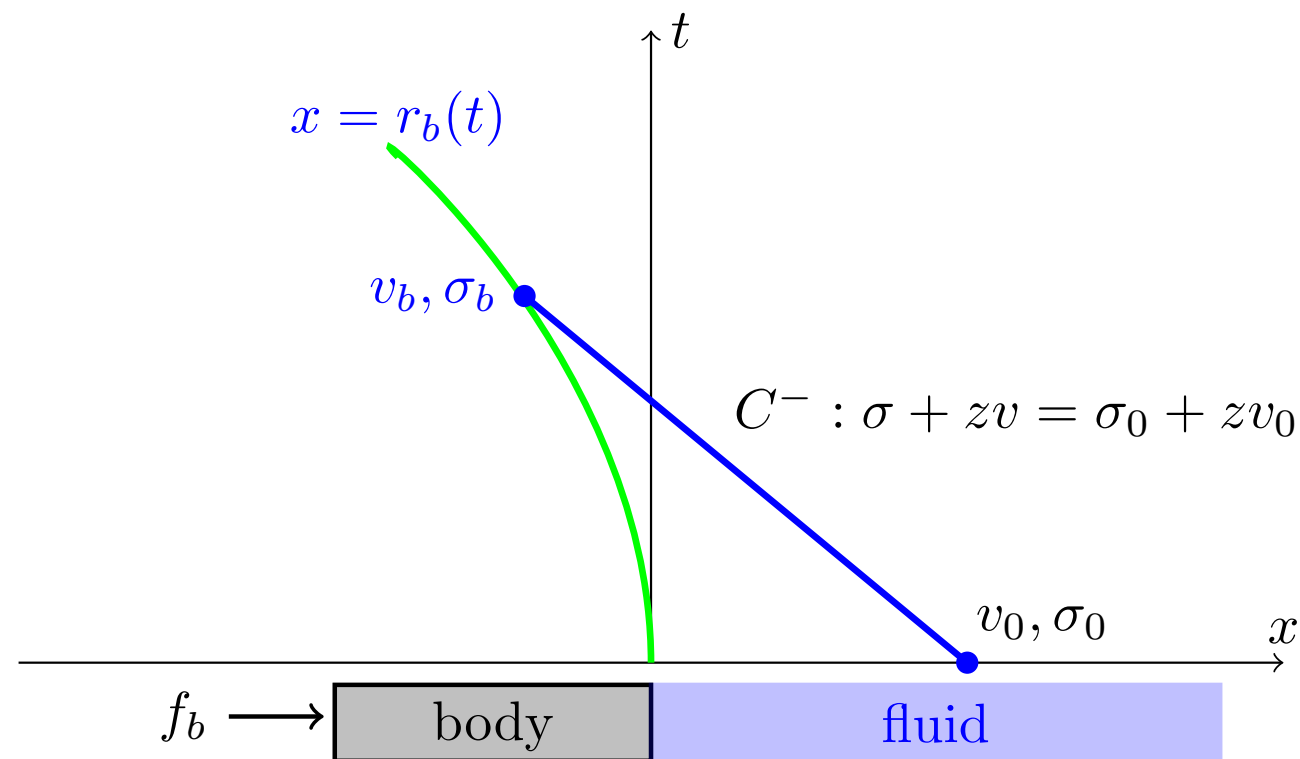
heavy solid
 $\bar{\rho} = 10.0$

The key lessons for the case of deforming bodies

- By embedding the solution to a local Riemann problem, we arrive at a stable partitioned FSI algorithm for compressible flow and deforming structures
 - Stability and accuracy can be proven and demonstrated
 - Overlapping grids are an efficient and powerful framework to implement the algorithm
- In some sense, the fact that the Riemann problem plays a key role is not surprising, and one major advance in this work was to show how to embed the solution via projection
- For the case of rigid bodies, it is not immediately obvious how to make use of these developments

$$v_I = \frac{\bar{z}\bar{v}_0 + zv_0}{\bar{z} + z} + \frac{\sigma_0 - \bar{\sigma}_0}{\bar{z} + z}$$
$$\sigma_I = \frac{\bar{z}^{-1}\bar{\sigma}_0 + z^{-1}\sigma_0}{\bar{z}^{-1} + z^{-1}} + \frac{v_0 - \bar{v}_0}{\bar{z}^{-1} + z^{-1}}$$

For rigid bodies the principle is the same, but the details are more subtle



Newton's law of motion

$$\begin{aligned} m_b \dot{v}_b &= \sigma_b + f_b, \\ \dot{x}_b &= v_b \end{aligned}$$

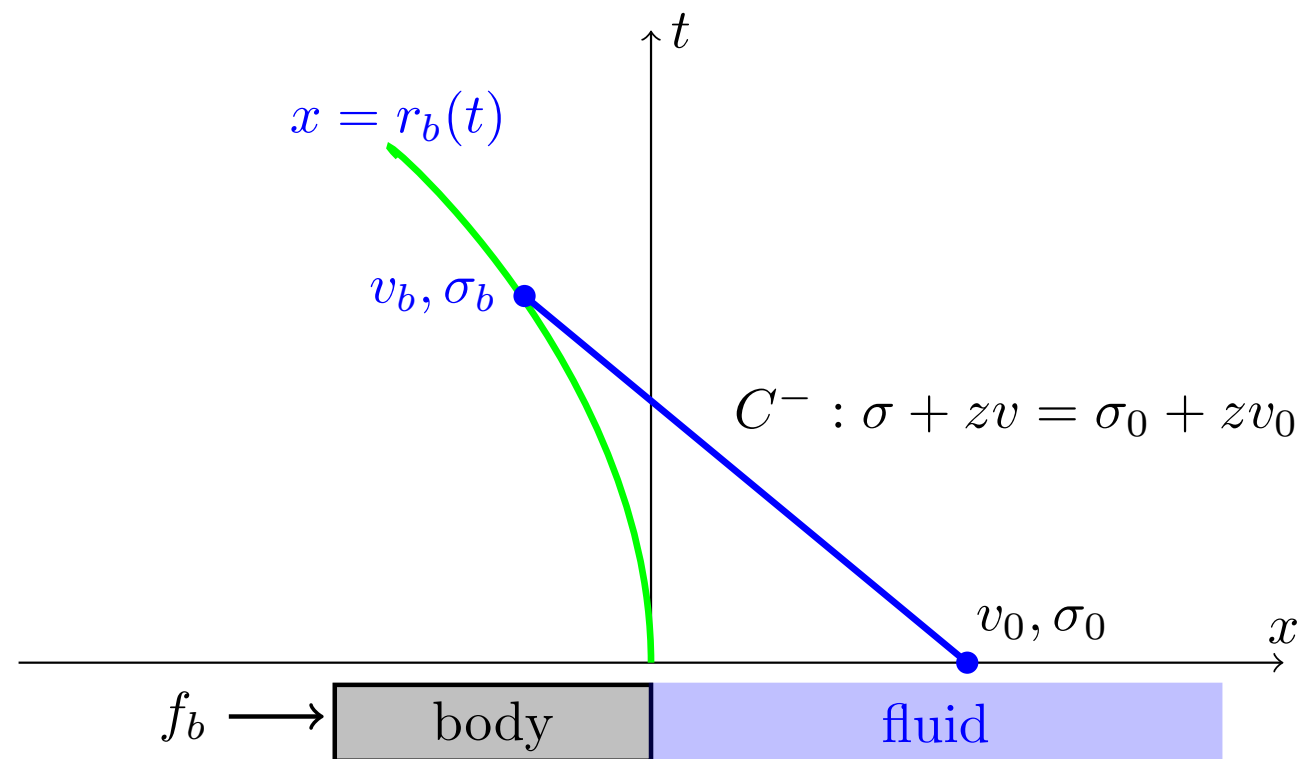
Linearized Euler equations

$$\begin{cases} \partial_t \rho + \hat{v} \partial_x \rho + \hat{\rho} \partial_x v = 0 \\ \partial_t v + \hat{v} \partial_x v - (1/\hat{\rho}) \partial_x \sigma = 0 \\ \partial_t \sigma + \hat{v} \partial_x \sigma - \hat{\rho} \hat{c}^2 \partial_x v = 0 \end{cases}$$

- From the theory of characteristics we obtain the stress on the body

$$\sigma_b = \sigma_0 + z(v_0 - v_b)$$

For rigid bodies the principle is the same, but the details are more subtle



Newton's law of motion

$$\begin{aligned} m_b \dot{v}_b &= \sigma_b + f_b, \\ \dot{x}_b &= v_b \end{aligned}$$

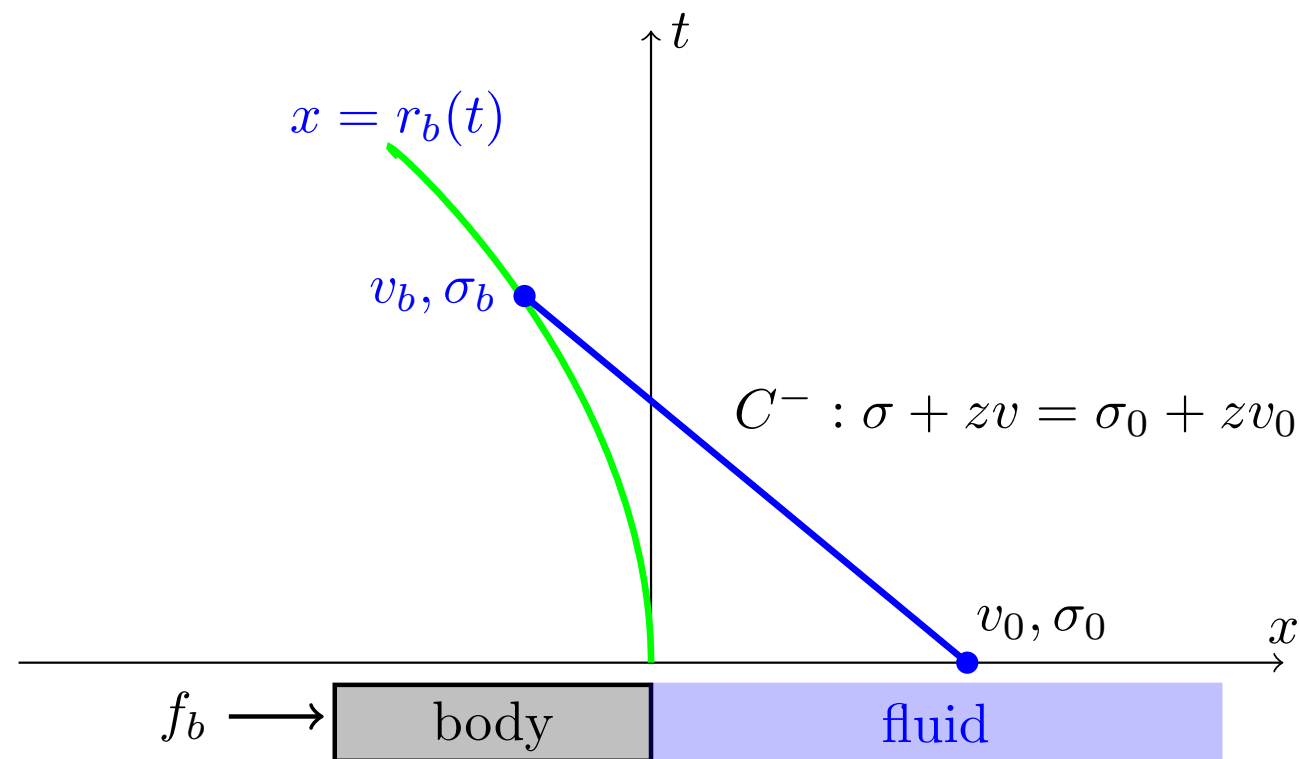
Linearized Euler equations

$$\begin{cases} \partial_t \rho + \hat{v} \partial_x \rho + \hat{\rho} \partial_x v = 0 \\ \partial_t v + \hat{v} \partial_x v - (1/\hat{\rho}) \partial_x \sigma = 0 \\ \partial_t \sigma + \hat{v} \partial_x \sigma - \hat{\rho} \hat{c}^2 \partial_x v = 0 \end{cases}$$

- From the theory of characteristics we obtain the stress on the body

$$\sigma_b = \sigma_0 + z(v_0 - v_b)$$

For rigid bodies the principle is the same, but the details are more subtle



Newton's law of motion

$$\begin{aligned} m_b \dot{v}_b &= \sigma_b + f_b, \\ \dot{x}_b &= v_b \end{aligned}$$

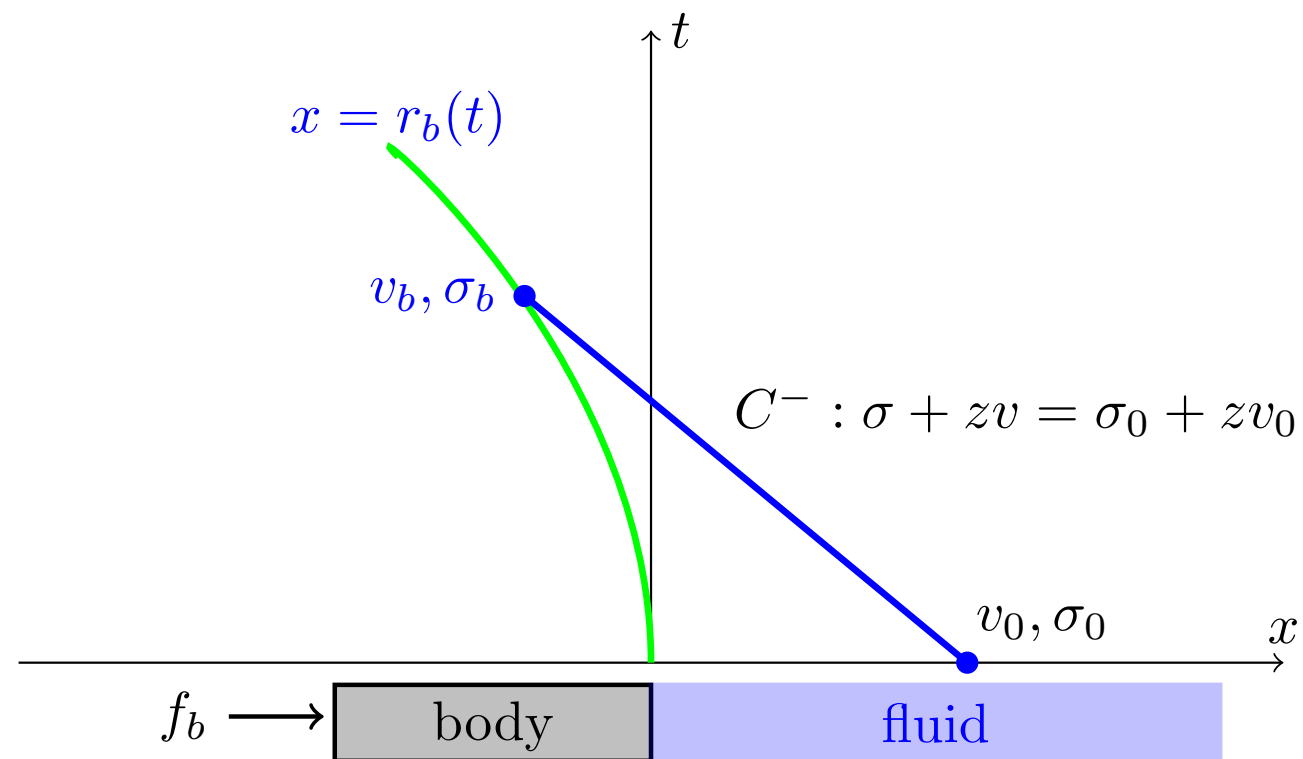
Linearized Euler equations

$$\begin{cases} \partial_t \rho + \hat{v} \partial_x \rho + \hat{\rho} \partial_x v = 0 \\ \partial_t v + \hat{v} \partial_x v - (1/\hat{\rho}) \partial_x \sigma = 0 \\ \partial_t \sigma + \hat{v} \partial_x \sigma - \hat{\rho} \hat{c}^2 \partial_x v = 0 \end{cases}$$

- From the theory of characteristics we obtain the stress on the body

$$\sigma_b = \sigma_0 + z(v_0 - v_b)$$

This stress projection is extremely important so I repeat it



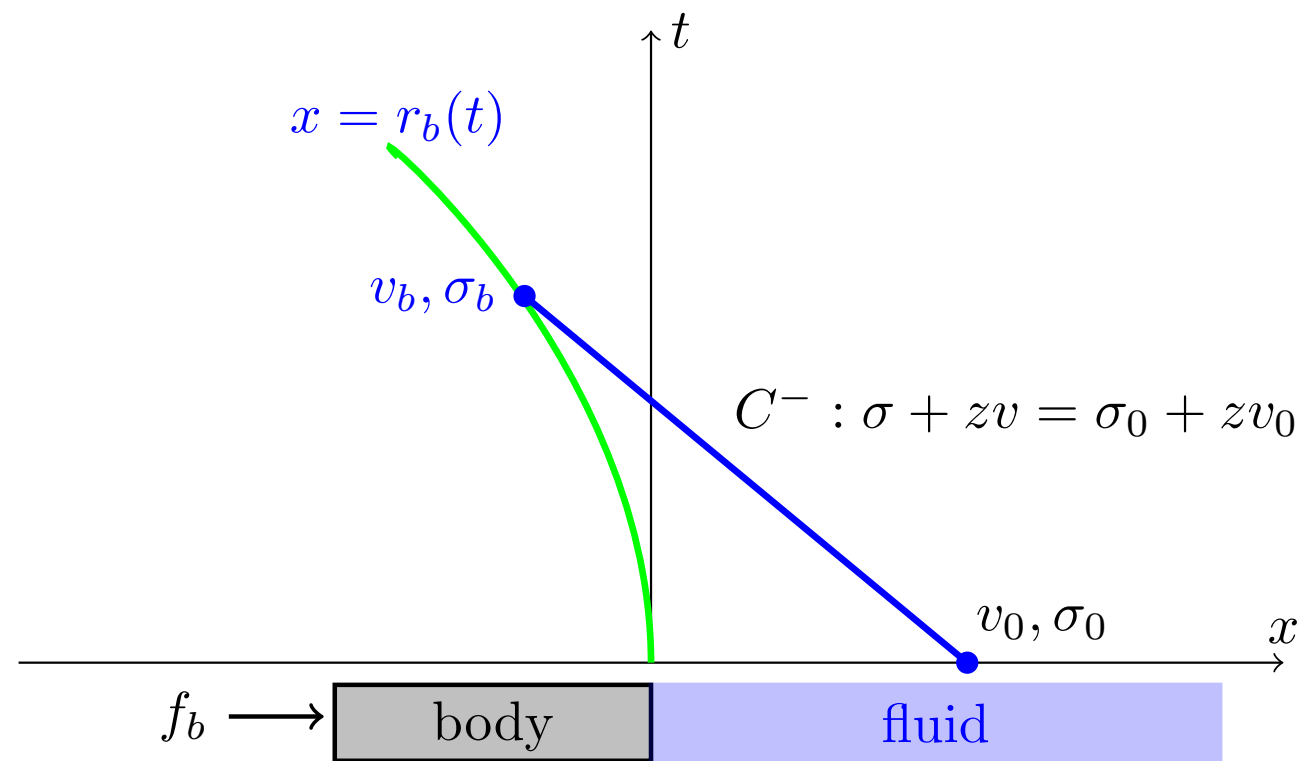
$$\sigma_b = \sigma_0 + z(v_0 - v_b)$$

- This says that the stress at the body depends on the velocity of the body
- Therefore the equations of motion are well-defined even for zero mass

$$m_b \dot{v}_b + zv_b = \sigma_0 + zv_0 + f_b(t)$$

- The added mass term occurs naturally and represents the mass of displaced fluid

This stress projection is extremely important so I repeat it



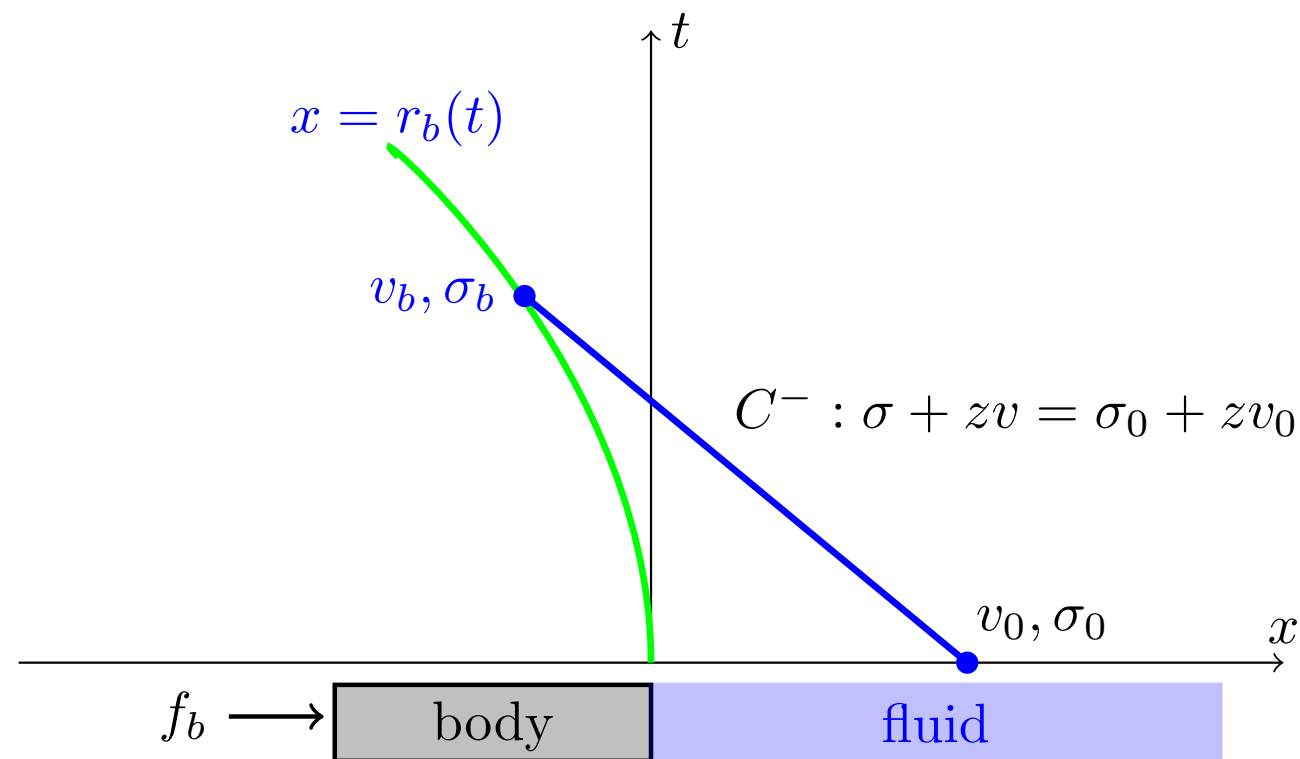
$$\sigma_b = \sigma_0 + z(v_0 - v_b)$$

- This says that the stress at the body depends on the velocity of the body
- Therefore the equations of motion are well-defined even for zero mass

$$m_b \dot{v}_b + z v_b = \sigma_0 + z v_0 + f_b(t)$$

- The added mass term occurs naturally and represents the mass of displaced fluid

This stress projection is extremely important so I repeat it



$$\sigma_b = \sigma_0 + z(v_0 - v_b)$$

- This says that the stress at the body depends on the velocity of the body
- Therefore the equations of motion are well-defined even for zero mass

$$m_b \dot{v}_b + \boxed{zv_b} = \sigma_0 + zv_0 + f_b(t)$$

- The added mass term occurs naturally and shows the effect of displaced fluid

Incorporating the projection in the 2D equations of motion is straight forward

- In 2D the equations of motion are

$$m_b \dot{\mathbf{v}}_b = \mathcal{F},$$
$$A \dot{\boldsymbol{\omega}} = -W A \boldsymbol{\omega} + \mathcal{T}$$

- Local projection of the stress on the surface of the body

$$\mathbf{f}_s(r) = -p_r \mathbf{n} = -p_f \mathbf{n} + z_f \left[\mathbf{n}^T (\mathbf{v}_f(r) - \mathbf{v}_b + \Xi \boldsymbol{\omega}) \right] \mathbf{n}$$

- Gives the applied forces and torques as

$$\mathcal{F} = \int_{\partial B} z_f \mathbf{n} \mathbf{n}^T (-\mathbf{v}_b + \Xi \boldsymbol{\omega}) ds + \int_{\partial B} -p_f \mathbf{n} + z_f (\mathbf{n}^T \mathbf{v}_f) \mathbf{n} ds + \mathbf{f}_b,$$
$$\mathcal{T} = \int_{\partial B} z_f \Xi \mathbf{n} \mathbf{n}^T (-\mathbf{v}_b + \Xi \boldsymbol{\omega}) ds + \int_{\partial B} \boldsymbol{\xi} \times (-p_f \mathbf{n} + z_f (\mathbf{n}^T \mathbf{v}_f) \mathbf{n}) ds + \mathbf{g}_b$$

- We have adopted the notation

$$W = \begin{bmatrix} 0 & -\omega_3 & \omega_2 \\ \omega_3 & 0 & -\omega_1 \\ -\omega_2 & \omega_1 & 0 \end{bmatrix} \quad \Xi = \begin{bmatrix} 0 & -\xi_3 & \xi_2 \\ \xi_3 & 0 & -\xi_1 \\ -\xi_2 & \xi_1 & 0 \end{bmatrix}$$

Incorporating the projection in the 2D equations of motion is straight forward

- In 2D the equations of motion are

$$m_b \dot{\mathbf{v}}_b = \mathcal{F},$$
$$A \dot{\boldsymbol{\omega}} = -W A \boldsymbol{\omega} + \mathcal{T}$$

- Local projection of the stress on the surface of the body

$$\mathbf{f}_s(r) = -p_r \mathbf{n} = -p_f \mathbf{n} + z_f \left[\mathbf{n}^T (\mathbf{v}_f(r) - \mathbf{v}_b + \Xi \boldsymbol{\omega}) \right] \mathbf{n}$$

- Gives the applied forces and torques as

$$\mathcal{F} = \int_{\partial B} z_f \mathbf{n} \mathbf{n}^T (-\mathbf{v}_b + \Xi \boldsymbol{\omega}) ds + \int_{\partial B} -p_f \mathbf{n} + z_f (\mathbf{n}^T \mathbf{v}_f) \mathbf{n} ds + \mathbf{f}_b,$$
$$\mathcal{T} = \int_{\partial B} z_f \Xi \mathbf{n} \mathbf{n}^T (-\mathbf{v}_b + \Xi \boldsymbol{\omega}) ds + \int_{\partial B} \boldsymbol{\xi} \times (-p_f \mathbf{n} + z_f (\mathbf{n}^T \mathbf{v}_f) \mathbf{n}) ds + \mathbf{g}_b$$

- We have adopted the notation

$$W = \begin{bmatrix} 0 & -\omega_3 & \omega_2 \\ \omega_3 & 0 & -\omega_1 \\ -\omega_2 & \omega_1 & 0 \end{bmatrix} \quad \Xi = \begin{bmatrix} 0 & -\xi_3 & \xi_2 \\ \xi_3 & 0 & -\xi_1 \\ -\xi_2 & \xi_1 & 0 \end{bmatrix}$$

Incorporating the projection in the 2D equations of motion is straight forward

- In 2D the equations of motion are

$$m_b \dot{\mathbf{v}}_b = \mathcal{F},$$
$$A \dot{\boldsymbol{\omega}} = -W A \boldsymbol{\omega} + \mathcal{T}$$

- Local projection of the stress on the surface of the body

$$\mathbf{f}_s(r) = -p_r \mathbf{n} = -p_f \mathbf{n} + z_f \left[\mathbf{n}^T (\mathbf{v}_f(r) - \mathbf{v}_b + \Xi \boldsymbol{\omega}) \right] \mathbf{n}$$

- Gives the applied forces and torques as

$$\mathcal{F} = \int_{\partial B} z_f \mathbf{n} \mathbf{n}^T (-\mathbf{v}_b + \Xi \boldsymbol{\omega}) ds + \int_{\partial B} -p_f \mathbf{n} + z_f (\mathbf{n}^T \mathbf{v}_f) \mathbf{n} ds + \mathbf{f}_b,$$
$$\mathcal{T} = \int_{\partial B} z_f \Xi \mathbf{n} \mathbf{n}^T (-\mathbf{v}_b + \Xi \boldsymbol{\omega}) ds + \int_{\partial B} \boldsymbol{\xi} \times (-p_f \mathbf{n} + z_f (\mathbf{n}^T \mathbf{v}_f) \mathbf{n}) ds + \mathbf{g}_b$$

- We have adopted the notation

$$W = \begin{bmatrix} 0 & -\omega_3 & \omega_2 \\ \omega_3 & 0 & -\omega_1 \\ -\omega_2 & \omega_1 & 0 \end{bmatrix} \quad \Xi = \begin{bmatrix} 0 & -\xi_3 & \xi_2 \\ \xi_3 & 0 & -\xi_1 \\ -\xi_2 & \xi_1 & 0 \end{bmatrix}$$

The resulting algorithm is very powerful and is provably stable for even the case of a zero mass rigid body

- The time stepping algorithm for generic overlapping grids is

The FSI time stepping algorithm			
Stage	Condition	Type	Assigns
Predict(a)	Predict body motion, moving grid	extrapolation	$\mathbf{x}_b^p, \mathbf{v}_b^p, \boldsymbol{\omega}^p, \mathbf{E}^p, \mathbf{G}_i^p$
Predict(b)	Advance fluid $\mathbf{w}_i^n, \mathbf{w}_i^p,$	PDE	$\mathbf{w}_i^n, \mathbf{i} \in \mathcal{I}_I, \mathbf{w}_i^p, \mathbf{i} \in \mathcal{I}_B$
Body(a)	Compute added mass terms		$A_{11}^p, A_{12}^p, A_{21}^p, A_{22}^p, \tilde{\mathcal{F}}^p, \tilde{\mathcal{T}}^p$
Body(b)	Advance rigid body	ODEs	$\mathbf{x}_b^n, \mathbf{v}_b^n, \boldsymbol{\omega}^n, \mathbf{E}^n$
Correct(a)	Project fluid on body	projection	$\mathbf{v}_i^n, p_i^n, \rho_i^n, \mathbf{i} \in \mathcal{I}_B$
Correct(b)	Correct moving grid	projection	\mathbf{G}_i^n
Ghost	Assign fluid ghost values	PDE, extrapolation	$\mathbf{w}_i^n, \mathbf{i} \in \mathcal{I}_G$

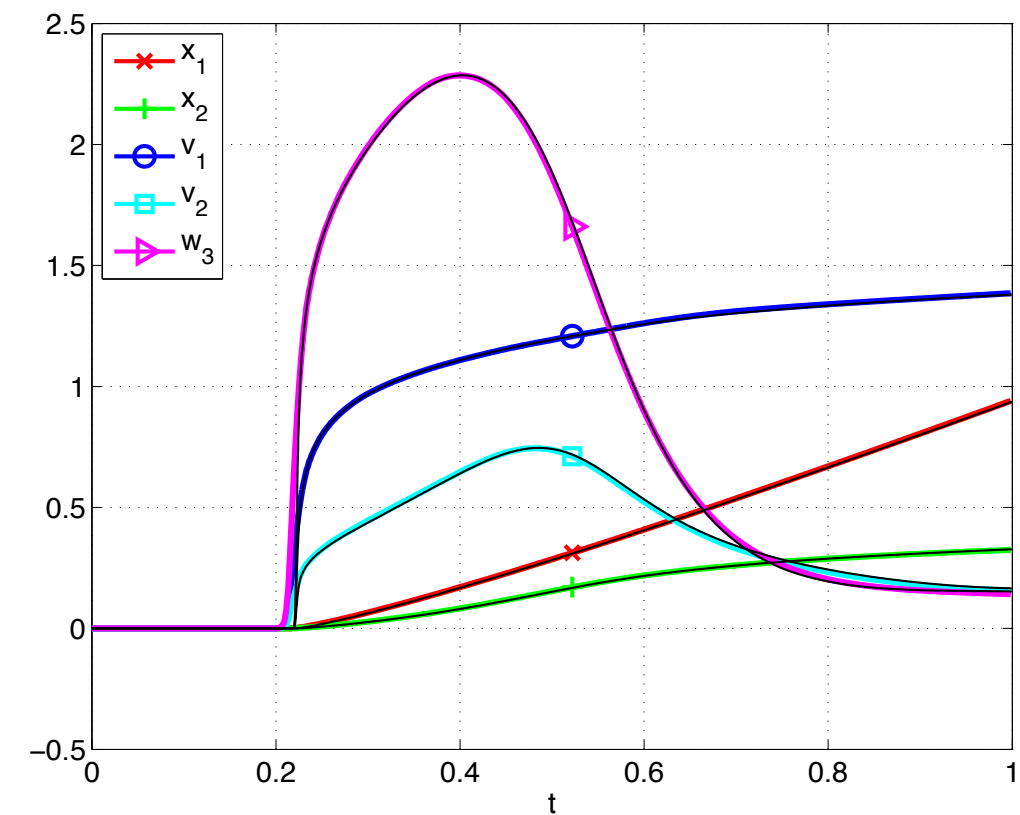
- Proofs of stability and detailed convergence analysis can be found at

JWB, WDH, B. Sjögreen, *A stable FSI algorithm for light rigid bodies in compressible flow*, LLNL-JRNL-558232, submitted

The resulting algorithm is very powerful and is provably stable for even the case of a zero mass rigid body

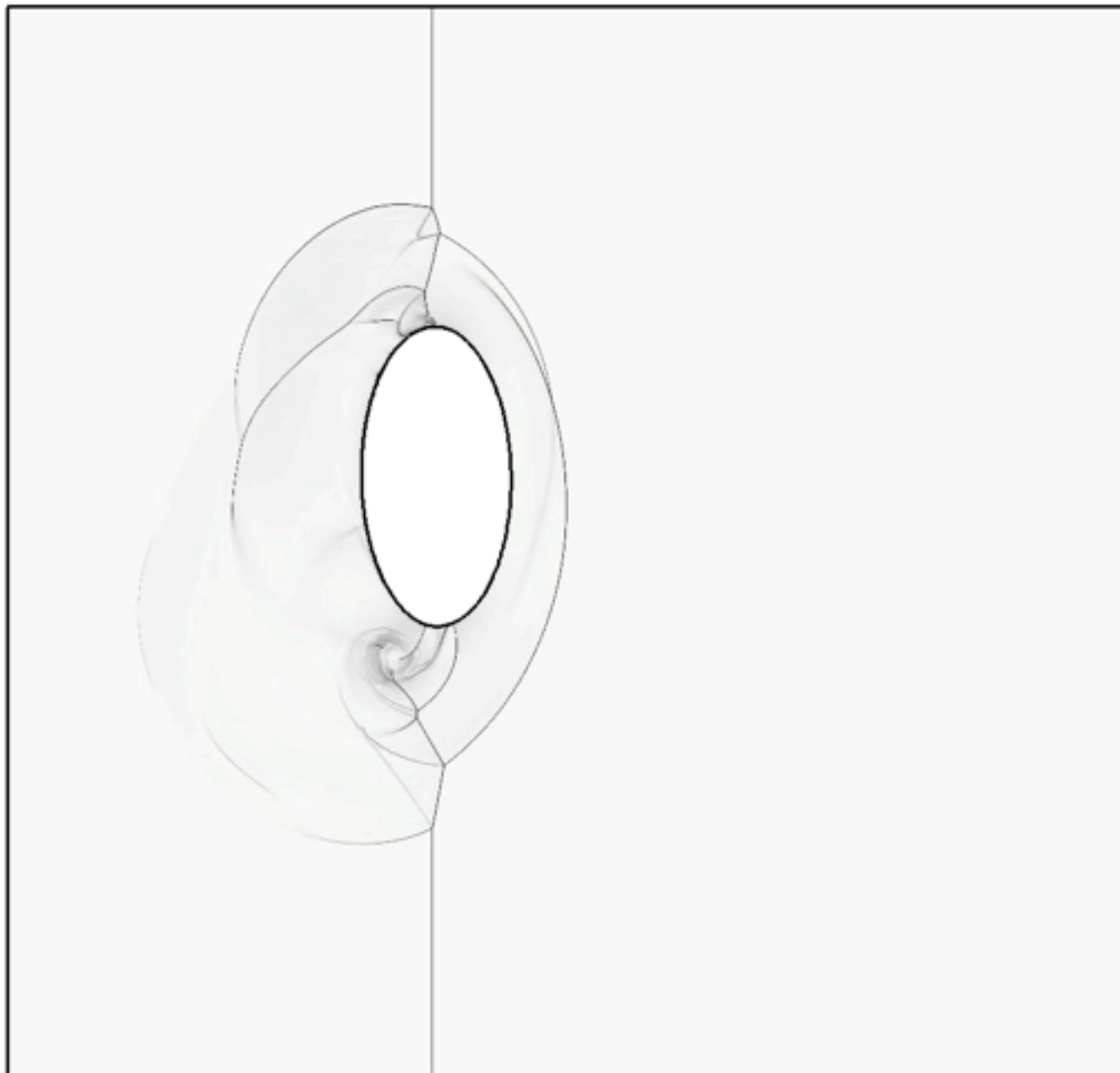
Mach 2 shock impacting zero mass body with AMR

Time histories of rigid body

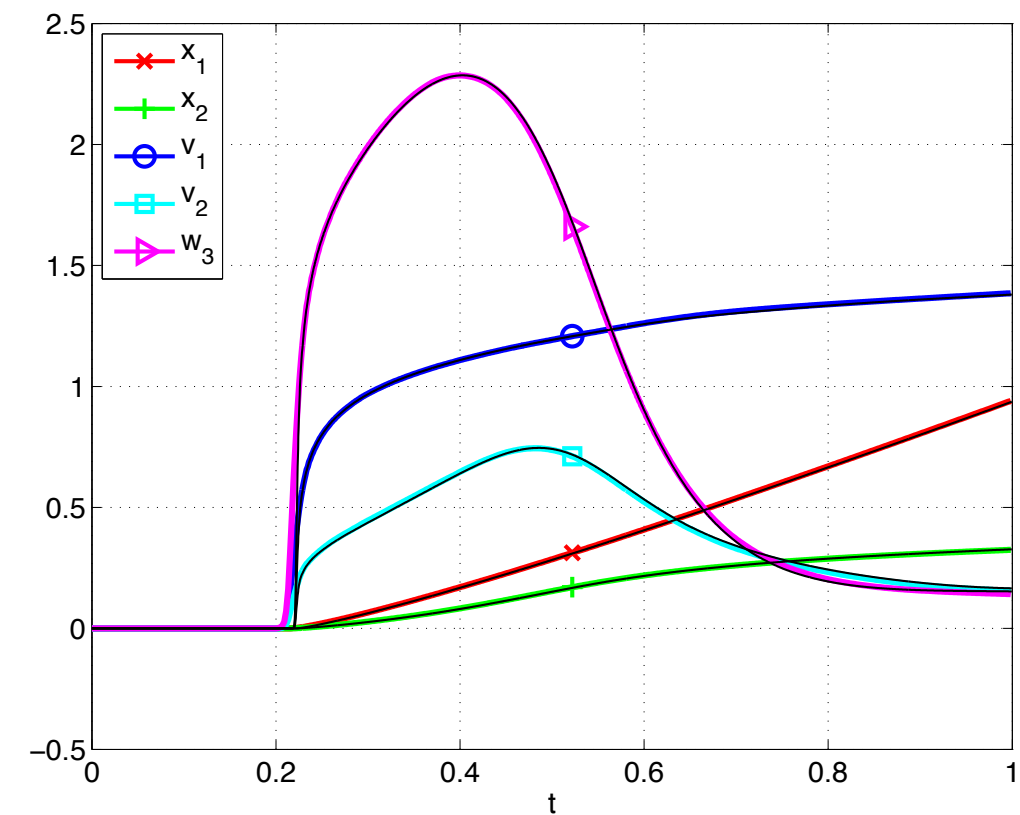


The resulting algorithm is very powerful and is provably stable for even the case of a zero mass rigid body

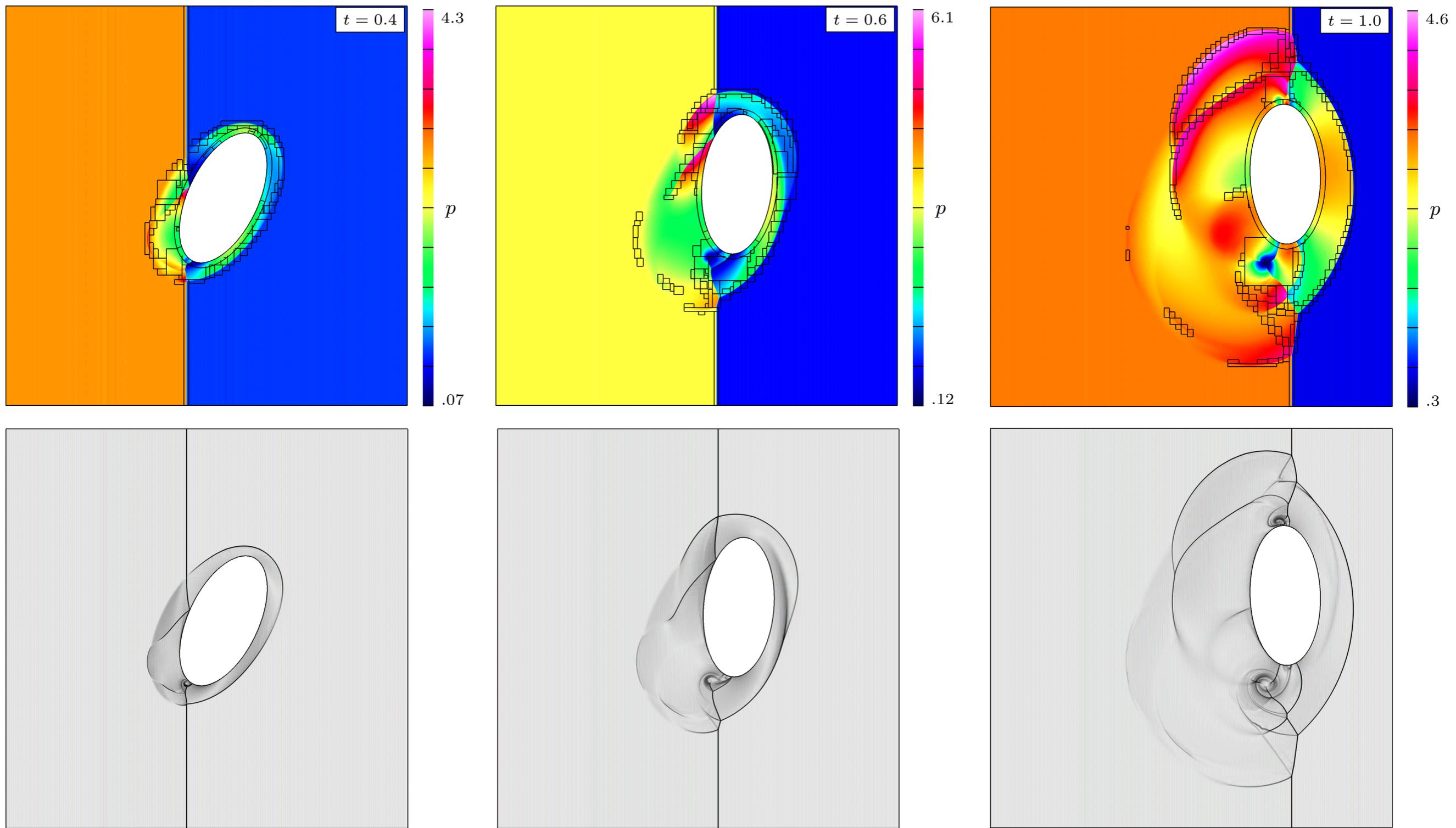
Mach 2 shock impacting zero mass body with AMR



Time histories of rigid body



The resulting algorithm is very powerful and is provably stable for even the case of a zero mass rigid body



JWB, WDH, B. Sjögreen, *A stable FSI algorithm for light rigid bodies in compressible flow*, LLNL-JRNL-558232, submitted

Summary

- The deforming composite grid approach was developed for coupling high-speed compressible fluids to elastic and rigid solids
- Stability was achieved for light and heavy solids using an interface projection technique which is motivated by the solution of simple local problems
- Analytic forms for the added mass tensors were derived
- Second-order convergence in the max-norm is verified for smooth flows

Future Work

- Move to more general solid models (nonlinear solids, beams, plates, etc ...)
- Extend analysis and methodology to incompressible fluids
- Move to three dimensions